

Journal of Visualized Experiments

Brain Infarct Segmentation and Registration on MRI or CT For Lesion-Symptom Mapping

--Manuscript Draft--

Article Type:	Invited Methods Article - JoVE Produced Video
Manuscript Number:	JoVE59653R2
Full Title:	Brain Infarct Segmentation and Registration on MRI or CT For Lesion-Symptom Mapping
Keywords:	lesion-symptom mapping; lesion-behavior mapping; infarct; stroke; segmentation; registration; image registration; spatial normalization; vascular cognitive impairment.
Corresponding Author:	J Matthijs Biesbroek Universitair Medisch Centrum Utrecht Utrecht, Utrecht NETHERLANDS
Corresponding Author's Institution:	Universitair Medisch Centrum Utrecht
Corresponding Author E-Mail:	J.M.Biesbroek@umcutrecht.nl
Order of Authors:	J Matthijs Biesbroek Hugo J Kuijf Nick A Weaver Lei Zhao Marco Duering Meta VCI Map consortium Geert Jan Biessels
Additional Information:	
Question	Response
Please indicate whether this article will be Standard Access or Open Access.	Standard Access (US\$2,400)
Please indicate the city, state/province, and country where this article will be filmed . Please do not use abbreviations.	Utrecht, Utrecht, the Netherlands

Utrecht, March 23, 2019

Concerning MS ID#: JoVE 59653

Dear professor Bajaj,

Thank you for giving us the opportunity to send you the revised version of our manuscript:
“Brain Infarct Segmentation and Registration on MRI or CT For Lesion-Symptom Mapping”.
We have revised the manuscript and addressed the editorial comments.

We hope you will find the revised paper suitable for publication in JoVE.

Yours sincerely,

Dr. J.M. Biesbroek

TITLE:

Brain Infarct Segmentation and Registration on MRI or CT for Lesion-Symptom Mapping

AUTHORS AND AFFILIATIONS:

J. Matthijs Biesbroek¹, Hugo J. Kuijf², Nick A. Weaver¹, Lei Zhao³, Marco Duering⁴, Geert Jan Biessels¹

¹Department of Neurology and Neurosurgery, UMC Utrecht Brain Center, University Medical Center Utrecht, Utrecht University, Utrecht, the Netherlands

²Image Sciences Institute, University Medical Center Utrecht, Utrecht, the Netherlands

³BrainNow Research Institute, Shenzhen, Guangdong Province, China

⁴Institute for Stroke and Dementia Research, University Hospital, LMU Munich, Munich, Germany

Corresponding Author:

J. Matthijs Biesbroek (j.m.biesbroek@umcutrecht.nl)

Email Addresses of Co-authors:

Hugo J. Kuijf (h.kuijf@umcutrecht.nl)

Zhao Lei (zhaolei@link.cuhk.edu.hk)

Nick A. Weaver (n.a.weaver@umcutrecht.nl)

Marco Duering (marco.duering@med.uni-muenchen.de)

Geert Jan Biessels (g.j.biessels@umcutrecht.nl)

KEYWORDS:

lesion-symptom mapping, lesion-behavior mapping, infarct, stroke, segmentation, registration, image registration, spatial normalization, vascular cognitive impairment

SUMMARY:

Provided here is a practical tutorial for an open-access, standardized image processing pipeline for the purpose of lesion-symptom mapping. A step-by-step walkthrough is provided for each processing step, from manual infarct segmentation on CT/MRI to subsequent registration to standard space, along with practical recommendations and illustrations with exemplary cases.

ABSTRACT:

In lesion-symptom mapping (LSM), brain function is inferred by relating the location of acquired brain lesions to behavioral or cognitive symptoms in a group of patients. With recent advances in brain imaging and image processing, LSM has become a popular tool in cognitive neuroscience. LSM can provide fundamental insights into the functional architecture of the human brain for a variety of cognitive and non-cognitive functions. A crucial step in performing LSM studies is the segmentation of lesions on brains scans of a large group of patients and registration of each scan to a common stereotaxic space (also called standard space or a standardized brain template). Described here is an open-access, standardized method for infarct segmentation and registration for the purpose of LSM, as well as a detailed and hands-

on walkthrough based on exemplary cases. A comprehensive tutorial for the manual segmentation of brain infarcts on CT scans and DWI or FLAIR MRI sequences is provided, including criteria for infarct identification and pitfalls for different scan types. The registration software provides multiple registration schemes that can be used for processing of CT and MRI data with heterogeneous acquisition parameters. A tutorial on using this registration software and performing visual quality checks and manual corrections (which are needed in some cases) is provided. This approach provides researchers with a framework for the entire process of brain image processing required to perform an LSM study, from gathering of the data to final quality checks of the results.

INTRODUCTION:

Lesion-symptom mapping (LSM), also called lesion-behavior mapping, is an important tool for studying the functional architecture of the human brain¹. In lesion studies, brain function is inferred and localized by studying patients with acquired brain lesions. The first case studies linking neurological symptoms to specific brain locations performed in the nineteenth century have already provided fundamental insights into the anatomical correlates of language and several other cognitive processes². Yet, the neuroanatomical correlates of many aspects of cognition or other brain functions remain elusive. In the past decades, improved structural brain imaging methods and technical advances have enabled large-scale in vivo LSM studies with high spatial resolution (i.e., at the level of individual voxels or specific cortical/subcortical regions of interest)^{1,2}. With these methodological advances, LSM has become an increasingly popular method in cognitive neuroscience and continues to offer new insights into the neuroanatomy of cognition and neurological symptoms³. A crucial step in any LSM study is the accurate segmentation of lesions and registration to a brain template. However, a comprehensive tutorial for the preprocessing of brain imaging data for the purpose of LSM is lacking.

Provided here is a complete tutorial for a standardized lesion segmentation and registration method. This method provides researchers with a pipeline for the standardized brain image processing and an overview of potential pitfalls that must be avoided. The presented image processing pipeline was developed through international collaborations⁴ and is part of the framework of the recently founded Meta VCI map consortium, whose purpose is performing multicenter lesion-symptom mapping studies in vascular cognitive impairment <www.metavcimap.org>⁵. This method has been designed to process both CT and MRI scans from multiple vendors and heterogeneous scan protocols to allow combined processing of imaging datasets from different sources. The required RegLSM software and all other software needed for this protocol is freely available except for MATLAB, which requires a license. This tutorial focuses on the segmentation and registration of brain infarcts, but this image processing pipeline can also be used for other lesions, such as white matter hyperintensities⁶.

Prior to initiating an LSM study, a basic understanding of the general concepts and pitfalls is required. Several detailed guidelines and a hitchhiker's guide are available^{1,3,6}. However, these reviews do not provide a detailed hands-on tutorial for the practical steps involved in gathering and converting brain scans to a proper format, segmenting the brain infarct, and registering the

scans to a brain template. The present paper provides such a tutorial. General concepts required for LSM are provided in the introduction with references for further reading on the subject.

General aim of lesion-symptom mapping studies

From the perspective of cognitive neuropsychology, brain injury can be used as a model condition to better understand the neuronal underpinnings of certain cognitive processes and to obtain a more complete picture of the cognitive architecture of the brain¹. This is a classic approach in neuropsychology that was first applied in post-mortem studies in the nineteenth century by pioneers like Broca and Wernicke². In the era of functional brain imaging, the lesion approach has remained a crucial tool in neuroscience because it provides proof that lesions in a specific brain region disrupt task performance, while functional imaging studies demonstrate brain regions that are activated during the task performance. As such, these approaches provide complementary information¹.

From the perspective of clinical neurology, LSM studies can clarify the relationship between the lesion location and cognitive functioning in patients with acute symptomatic infarcts, white matter hyperintensities, lacunes, or other lesion types (e.g., tumors). Recent studies have shown that such lesions in strategic brain regions are more relevant in explaining cognitive performance than global lesion burden^{2,5,7,8}. This approach has the potential to improve understanding of the pathophysiology of complex disorders (in this example, vascular cognitive impairment) and may provide opportunities for developing new diagnostic and prognostic tools or supporting treatment strategies².

LSM also has applications beyond the field of cognition. In fact, any variable can be related to lesion location, including clinical symptoms, biomarkers, and functional outcome. For example, a recent study determined infarct locations that were predictive of functional outcome after ischemic stroke¹⁰.

Voxel-based versus region of interest-based lesion-symptom mapping

To perform lesion-symptom mapping, lesions need to be segmented and registered to a brain template. During the registration procedure, each patient's brain is spatially aligned (i.e., normalized or registered to a common template) to correct for differences in brain size, shape, and orientation so that each voxel in the lesion map represents the same anatomical structure for all patients⁷. In standard space, several types of analyses can be performed, which are briefly summarized here.

A crude lesion-subtraction analysis can be performed to show the difference in lesion distribution in patients with deficits compared to patients without deficits. The resulting subtraction map shows regions that are more often damaged in patients with deficits and spared in patients without deficits¹. Though a lesion-subtraction analysis can provide some insights into correlates of a specific function, it provides no statistical proof and is now mostly used when the sample size is too low to provide enough statistical power for voxel-based lesion-symptom mapping.

In voxel-based lesion-symptom mapping, an association between the presence of a lesion and cognitive performance is determined at the level of each individual voxel in the brain (**Figure 1**). The main advantage of this method is the high spatial resolution. Traditionally, these analyses have been performed in a mass-univariate approach, which warrants correction for multiple testing and introduces a spatial bias caused by inter-voxel correlations that are not taken into account^{1,10,11}. Recently developed approaches that do take inter-voxel correlations into account (usually referred to as multivariate lesion-symptom mapping methods, such as Bayesian analysis¹³, support vector regression^{4,14}, or other machine learning algorithms¹⁵) show promising results and appear to improve the sensitivity and specificity of findings from voxel-wise LSM analyses compared to traditional methods. Further improvement and validation of multivariate methods for voxel-wise LSM is an ongoing process. The best method choice for specific lesion-symptom mapping depends on many factors, including the distribution of lesions, outcome variable, and underlying statistical assumptions of the methods.

In the region of interest (ROI)-based lesion-symptom mapping, an association between the lesion burden within a specific brain region and cognitive performance is determined (see Figure 1 in Biesbroek et al.² for an illustration). The main advantage of this method is that it considers the cumulative lesion burden within an anatomical structure, which in some cases may be more informative than a lesion in a single voxel. On the other hand, ROI-based analyses have limited power for detecting patterns that are only present in a subset of voxels in the region¹⁶. Traditionally, ROI-based lesion-symptom mapping is performed using logistic or linear regression. Recently, multivariate methods that deal better with collinearity have been introduced (e.g., Bayesian network analysis¹⁷, support vector regression^{4,18}, or other machine learning algorithms¹⁹), which may improve the specificity of findings from lesion-symptom mapping studies.

Patient selection

In LSM studies, patients are usually selected based on a specific lesion type (e.g., brain infarcts or white matter hyperintensities) and the time interval between diagnosis and neuropsychological assessment (e.g., acute vs. chronic stroke). The optimal study design depends on the research question. For example, when studying the functional architecture of the human brain, acute stroke patients are ideally included because functional reorganization has not yet occurred in this stage, whereas chronic stroke patients should be included when studying the long-term effects of stroke on cognition. A detailed description of considerations and pitfalls in patient selection is provided elsewhere⁷.

Brain image preprocessing for the purpose of lesion-symptom mapping

Accurate lesion segmentation and registration to a common brain template are crucial steps in lesion-symptom mapping. Manual segmentation of lesions remains the gold standard for many lesion types, including infarcts⁷. Provided is a detailed tutorial on criteria for manual infarct segmentation on CT scans, diffusion weighted imaging (DWI), and fluid-attenuated inversion recovery (FLAIR) MRI sequences in both acute and chronic stages. The segmented infarcts (i.e., the 3D binary lesion maps) need to be registered before any across-subject analyses are

performed. This protocol uses the registration method RegLSM, which was developed in a multicenter setting⁴. RegLSM applies linear and non-linear registration algorithms based on elastix²⁰ for both CT and MRI, with an additional CT processing step specifically designed to enhance registration quality of CT scans²¹. Furthermore, RegLSM allows for using different target brain templates and an (optional) intermediate registration step to an age-specific CT/MRI template²². The possibility of processing both CT and MRI scans and its customizability regarding intermediate and target brain templates makes RegLSM a highly suitable image processing tool for LSM. The entire process of preparing and segmenting CT/MRI scans, registration to a brain template, and manual corrections (if required) are described in the next section.

[Place **Figure 1** here]

PROTOCOL

This protocol follows the guidelines of our institutions human research ethics committee.

1. Collection of scans and clinical data

1.1. Collect brain CT or MRI scans of patients with ischemic stroke. Most scanners save the scans as DICOM (Digital Imaging and Communications in Medicine) files that can be copied to a hard disk or server.

NOTE: Scans from every scanner type, scan protocol, and MRI field strength can be used, as long as 1) the time window requirements for the used scan type are met (see **Table 1**) and 2) there are no artifacts that hamper accurate infarct delineation. A detailed tutorial on artifact detection on CT and MRI is provided elsewhere^{23,24}. An example of commonly occurring motion artifacts on CT is provided in **Figure 2**, and examples of scans of good quality are provided in the exemplar cases in the results section. Infarcts can be segmented on scans with any slice thickness and any in-plane image resolution. However, thin slices and high in-plane resolution will enable a more accurate representation of the infarct to the brain template.

1.2. Collect the clinical variables in a data file (e.g., Excel) by making separate rows for each case and columns for each clinical variable. For infarct segmentation, include at least the variables date of stroke and date of imaging or a variable that indicates the time interval between stroke and imaging.

1.3. Ensure that ethical guidelines and regulations regarding privacy are followed. Ensure that the data is either anonymized or coded. Pay specific attention to the removal of patient data such as name, address, and date of birth that are stored in the DICOM files as tags. These tags can be cleared using dcm2niix (free download available at <https://github.com/rordenlab/dcm2niix>)²⁵.

2. Conversion of DICOM images to nifti files

2.1. To convert the DICOM images to uncompressed nifti files using the dcm2niix tool, type “[folder path of dcm2niix.exe]\dcm2niix %d_%p [folder path of dicom files]” in the command prompt. An example of the command with the folders paths inserted could be C:\users\matthijs\dcm2niix %d_%p C:\users\matthijs\dicom\. This command will run the dcm2niix executable, convert the DICOM images in the selected folder and save the nifti files in the same folder.

NOTE: The addition %d_%p ensures that the series description and protocol name are inserted in the file name. Additional features including options for batch conversion are provided in the dcm2niix manual at <<https://www.nitrc.org/plugins/mwiki/index.php/dcm2nii:MainPage>>. Other open source tools can be used for the conversion of DICOM images to nifti files, as well.

2.2. Ensure that the name of the scan type (CT, FLAIR, DWI, or other sequence names) is copied into the file name during conversion (this option is available in dcm2niix).

2.3 For MRI scans, select DWI or FLAIR sequences for segmentation. Alternatively, any other structural sequence on which the infarct is visible can be used. See **Table 1** for appropriate time windows after stroke in which CT, DWI, or FLAIR can be used for infarct segmentation.

2.4. Organize the nifti files in a convenient folder structure with a subfolder for each case (see the manual of RegLSM and **Supplementary Figure 1**). This manual can be downloaded from <www.metavcimap.org/support/software-tools>.

NOTE: This folder structure is a requirement for the registration software RegLSM (see section 4). An update of RegLSM, making it BIDS (brain imaging data structure²⁶, see <<http://bids.neuroimaging.io>>) compatible, is currently being developed and will soon be released.

3. Infarct segmentation

3.1. General remarks applying to all scan types

3.1.1. Ensure that the person who performs and evaluates segmentation and registration is blinded to the outcome variable (usually a cognitive measure) to avoid bias.

3.1.2. Note that infarcts are usually segmented on transversal slices, but segmentation can be performed in any slice orientation.

3.1.3. Ensure ideal viewing conditions during infarct segmentation by using a high-resolution monitor display and optimal ambient light to provide a comfortable setting. Manually adjust the image contrast during segmentation to provide optimal contrast between healthy brain tissue. Be consistent in applying similar settings across subjects.

3.2. Infarct segmentation on CT

3.2.1 First check whether the scan was performed at least 24 h after stroke symptom onset. Within 24 h, the acute infarct is not or only partially visible on CT and the scan cannot be used for segmentation⁷. See **Figure 3** for an illustration.

3.2.2 Open the native CT using ITK-SNAP software (free download available at www.itksnap.org)²⁷. In ITK-SNAP, click **File | open main image** from the dropdown menu. Click **browse** and select the file to open the scan. If the default contrast setting provides poor contrast between healthy brain tissue and the lesion, adjust the contrast settings. To do so, click **Tools | image contrast | contrast adjustment**.

NOTE: Any open source software can also be used.

3.2.3 If available, open a CT that was performed within 24 h after stroke symptom onset in a separate instance as the reference to distinguish the acute infarct from old ischemic lesions such as lacunes, (sub)cortical infarcts, or white matter hyperintensities.

3.2.4. Identify the infarct based on the following characteristics. Infarcts have a low signal (i.e., hypodense) compared to normal brain tissue.

3.2.4.1. Consider the infarcts to be in the acute stage (first weeks) if there are large infarcts that can cause mass effect resulting in the displacement of surrounding tissues, compression of ventricles, midline shift, and obliteration of sulci. Check for the presence of hemorrhagic transformation, which is visible as regions with high signal (i.e., hyperdense) within the infarct.

3.2.4.2. Consider the infarcts to be in the chronic stage (months to years) if the infarct consists of a hypodense cavitated center (with a similar density as the cerebrospinal fluid) and less hypodense rim, which represents damaged brain tissue. Segment both the cavitated center and hypodense rim as an infarct. In case of large infarct, there can be ex vacuo enlargement of adjacent sulci or ventricles.

NOTE: Tissue displacement due to mass effect or ex vacuo enlargement of structures should not be corrected for during segmentation (i.e., only the full extent of the infarct has to be segmented). Correction for tissue displacement takes place during the registration and subsequent steps.

3.2.5 Segment the infarcted brain tissue using the **paintbrush mode** from the main toolbar (left-click to draw, right-click to erase). Alternatively, use the **polygon mode** to place anchor points at the borders of the lesion (these points are automatically connected with lines) or hold the left mouse button while moving the mouse over the borders of the lesion. Once all anchor points are connected, click **accept** to fill the delineated area.

3.2.6. Avoid the fogging phase, which refers to the phase in which the infarct becomes isodense on CT (which co-occurs with infiltration of the infarcted tissue with phagocytes). This typically

occurs 14–21 days after stroke onset, but in rare cases can occur even earlier²⁸. During this period, the infarct can become invisible or its boundaries become less clear, making this stage unsuitable for infarct segmentation. After the fogging phase, the lesion becomes hypodense again when cavitation and gliosis occur. See **Figure 4** for two examples.

3.2.7. After finishing the segmentation, save it as a binary nifti file in the same folder as the scan by clicking **segmentation | save segmentation image** from the dropdown menu, then save the segmentation by giving it the exact same name as the segmented scan, with the extension of .lesion (e.g., if the scan was saved as “ID001.DWI.nii”, save the segmentation as “ID001.DWI.lesion.nii”).

3.3 Infarct segmentation on DWI

3.3.1. First check if the DWI was performed within 7 days of stroke onset. Infarcts are visible on DWI within several hours after stroke onset and their visibility on DWI gradually decreases after approximately 7 days (see paragraph 2 in the discussion for more details).

3.3.2 Open the DWI in ITK-SNAP (in the same way as done in step 3.2.2).

NOTE: A DWI sequence generates at least two images for most scan protocols, one with a b-value = 0, which is a standard T2-weighted image, and one with a higher b-value, which is the scan that captures the actual diffusion properties of the tissue. The higher the b-value, the stronger the diffusion effects. For ischemic stroke detection, a b-value around 1000 s/mm² is often used, as this provides a good contrast-to-noise ratio in most cases²⁹. The image with a high b-value is used for infarct segmentation.

3.3.3 Open the apparent diffusion coefficient (ADC) sequence in a separate instance of ITK-SNAP for reference.

3.3.4. Identify and annotate the infarcted brain tissue based on the high signal (i.e., hyperintense) on DWI and low signal (i.e., hypointense) on the ADC (see **Figure 5**). ADC values in the infarct gradually increase until ADC normalizes to average, 1 week after the stroke³⁰, but in some cases, the ADC may already be (nearly) normalized after several days if there is much vasogenic edema (see step 3.2.5).

NOTE: In DWI images with low b-values, brain lesions with an intrinsic high T2 signal (such as white matter hyperintensities) can also appear hyperintense. This phenomenon is called T2 shine-through³¹. However, with increasing b-values, this phenomenon becomes less relevant, as the signal on the DWI image more strongly reflects diffusion properties instead of intrinsic T2 signal. With modern DWI scan protocols (usually with b-value=1000 or higher), the T2 shine-through effects are limited³².

3.3.5. Do not mistake a high DWI signal near interfaces between air and either tissue or bone, which are a commonly observed artifact, for an infarct. See **Figure 5**.

3.3.6. Save the annotation as a binary nifti file, giving it the exact same name as the segmented scan, with the extension of .lesion (in the same way as done in step 3.2.7).

3.4. Infarct segmentation on FLAIR

3.4.1. First, check if the scan was performed >48 h after stroke symptom onset. In the hyperacute stage, the infarct is usually not visible on the FLAIR sequence or the exact boundaries of the infarct are unclear³¹ (see **Figure 6**).

3.4.2. Open the FLAIR in ITK-SNAP in the same way as done in step 3.2.2.

3.4.3. Open the T1 a separate instance of ITK-SNAP for reference, if available.

3.4.4. Identify and segment the infarcted brain tissue based on the following characteristics.

3.4.4.1. Annotate the tissue in the acute stage (within the first few weeks), if the infarct is visible as a homogeneous hyperintense lesion, with or without apparent swelling and mass effect (**Figure 5**).

3.4.4.2. Annotate the tissue in the chronic stage (months to years) if the infarct is cavitated (i.e., the center becomes hypo- or iso-intense on FLAIR). Identify this cavity on the T1. In most cases, the cavitated center is surrounded by a hyperintense rim on the FLAIR, representing gliosis³³.

NOTE: However, there is a considerable amount of variation in the degree of cavitation and gliosis of chronic infarcts. Segment both the cavity and the hyperintense rim as infarcts (see step 3.2.5). A FLAIR hyperintense lesion is not always an infarct. In the acute stage, small subcortical infarcts can easily be distinguished from white matter hyperintensities or other chronic lesions such as lacunes of presumed vascular origin when there is a DWI available (see **Figure 5**). In the chronic stage, it can be more difficult. See paragraph 3 in the discussion for more information on how to discriminate these lesion types in the chronic stage.

3.4.5. Save the annotation as a binary nifti file, giving it the exact same name as the segmented scan, with the extension of .lesion (in the same way as done in step 3.2.7).

[Place **Table 1** here].

4. Registration to standard space

4.1. Download RegLSM from <www.metavcimap.org/features/software-tools>⁴. Use this tool to process CT scans and any kind of MRI sequence. The registration procedure is illustrated in **Figure 7**.

NOTE: Optional features in RegLSM include registration to an intermediate CT/MRI template

that more closely resembles the scans of older patients with brain atrophy²². By default, the CT and MRI scan are registered to the MNI-152 template³⁴, but this can be replaced by other templates if this better suits the study. Different registration schemes are illustrated in **Figure 7**. Other open source registration tools can also be used for this step.

4.2. Check 1) if the nifti files are not compressed, 2) that the file name of the segmented scan contains the term CT, FLAIR, or DWI, and 3) that the file name of the lesion annotation contains the same term with an appended “.lesion”. If these first three steps are followed, the data is fully prepared for registration and nothing needs to be changed.

4.3. Open MATLAB (version 2015a or higher), set the current folder to **RegLSM** (this folder can be downloaded from www.metavcimap.org), and enable SPM³⁵ (version 12 or higher, free download at <https://www.fil.ion.ucl.ac.uk/spm/>) by typing **addpath** {folder name of SPM}. Next, type **RegLSM** to open the GUI.

4.4. Select **test mode** in the registration dropdown menu to perform the registration for a single case. In the test mode panel, select the scan (CT, FLAIR, or DWI), annotation, and optionally the T1, using the **open image** button. Select the registration scheme: **CT, FLAIR with or without T1, DWI with or without T1**.

4.5. Alternatively, select **batch mode** to register the scans of all cases in the selected folder in batch mode.

4.6. Ensure that RegLSM saves the resulting registration parameters and the registered scans (including intermediate steps) and the registered lesion map in subfolders that are automatically generated. During this process, the registered scans and lesion maps are resampled to match the resolution (isotropic 1 mm³ voxels) and angulation of the MNI-152 template.

5. Review registration results

5.1. Select the option **check results** in the RegLSM GUI and browse to the main folder with the registration results. The GUI will automatically select the registered scan with the registered lesion map, and the MNI-152 template with the registered lesion map in transverse, sagittal, and coronal orientations (see **Figure 8**).

5.2. Scroll through the registered scan and use the crosshair to check the alignment of the registered scan and the MNI-152 template. Pay specific attention to the alignment of recognizable anatomical landmarks such as the basal ganglia, ventricles, and skull.

5.3. Mark all failed registrations in a separate column in the data file (made in step 1.2) for the subsequent manual correction in section 6.

NOTE: Common errors in the registration are imperfect alignment due to the mass effect

caused by the lesion in the acute stage, or ex vacuo enlargement of ventricles in the chronic stage. See **Figure 3** and **Figure 5** for examples of such misalignment. Another common error is a misalignment of the tentorium cerebelli, in which case an occipital infarct can overlap with the cerebellum in the template. Misalignment of tissues that are not lesioned is not an issue when only the binary lesion maps are used in the subsequent lesion-symptom mapping analyses. In such cases, only the lesions need to be perfectly aligned.

6. Manually correct registration errors

6.1. For the lesion maps that need correction, open the MNI-152 T1 template in ITK-SNAP and select from the **segmentation** menu | **open segmentation** | **registered lesion map**, which is now overlaid on the template.

6.2. In RegLSM, open the results for the reference, as explained in step 5.1.

6.3. Correct the registered lesion map in ITK-SNAP for any type of misalignment that is mentioned in step 5.3 using the **brush function** to add voxels (left click) or remove voxels (right click). Carefully compare the registered scan and overlaid lesion map (see step 5.2) with the MNI-152 template and overlaid lesion map in ITK-SNAP (see step 6.1) to identify the regions of misalignment. See **Figure 3** and **Figure 5**.

6.4. After manually correcting lesion map in MNI space, perform a final check by comparing the segmented native scan of the patient with the corrected lesion map in MNI space (i.e., the results of step 6.3). Ensure that the corrected lesion map in MNI space now accurately represents the infarct in native space. Pay specific attention to the recognizable landmarks such as basal ganglia, ventricles, and skull (similar to step 5.2).

6.5. Save the corrected lesion map in MNI space as a binary nifti file in the same folder as the uncorrected lesion map in MNI-152 space, giving it the exact same name as the uncorrected lesion map, with the extension of .corrected.

7. Preparing data for lesion-symptom mapping

7.1. Rename all the lesion maps. By default, RegLSM saved the lesion maps in a subfolder with the file name “results”. Include the subject ID in the file name. In the case of manual correction, be sure to select and rename the corrected file.

7.2 Copy all the lesion maps into a single folder.

7.3 Perform a sanity check of the data by randomly selecting and inspecting several lesion maps in ITK-SNAP and compare these with the native scans to rule out systematic errors in data processing such as left-right flipping.

7.4 Use MRICron <<https://www.nitrc.org/projects/mricron>> to perform another sanity check of

the data by creating a lesion overlap image to check if no lesions are located outside the brain template. Do this by selecting the **draw** dropdown menu | **statistics** | **create overlap images**.

NOTE: The resulting lesion overlay map can be projected on the MNI-152 template and inspected using, for example, MRICron or ITK-SNAP.

7.5 Ensure that the lesion maps are now ready to be used for voxel-based lesion-symptom mapping or for calculation of infarct volumes within specific regions of interest using an atlas that is registered to the same standard space as the lesion maps (in this case, MNI-152 space for which many atlases are available, only a few of which are cited below^{36–38}).

REPRESENTATIVE RESULTS:

Exemplar cases of brain infarct segmentations on CT (**Figure 3**), DWI (**Figure 5**), and FLAIR (**Figure 6**) images, and subsequent registration to the MNI-152 template are provided here. The registration results shown in **Figure 3B** and **Figure 5C** were not entirely successful, as there was misalignment near the frontal horn of the ventricle. The registered lesion maps of these unsuccessful registrations were manually corrected, the results of which are shown in the figures. After this manual correction, the lesion maps of each of these three exemplary cases are an accurate representation of the infarcts in native space, and the lesion maps are ready to be used for subsequent lesion-symptom mapping. **Figure 6C** show an example of an adequate registration result that does not require any manual correction.

These figures also highlight several potential pitfalls in brain infarct segmentation on each of these scan modalities. **Figure 2** shows an example of motion artifacts on a CT scan, in which case the patient should be excluded from LSM studies. **Figure 4** shows an example of fogging on a CT scan, which typically occurs 14–21 days after stroke, leading to an underestimation of the infarct size. CT scans made in this time interval should therefore not be used for lesion-symptom mapping. **Figure 7** shows the results of three typical brain image registration schemes generated using the RegLSM software. **Figure 8** shows the results of the registration of a DWI image to the MNI-152 T1 template in the RegLSM registration result viewer.

These results illustrate the entire process of infarct segmentation on CT and MRI, registration to standard space, subsequent quality checks, and when necessary, the manual correction of the registration results. The resulting lesion maps are ready to be used in voxel-based or region of interest-based lesion-symptom mapping.

[Place Figure 2 here]

[Place Figure 3 here]

[Place Figure 4 here]

[Place Figure 5 here]

[Place Figure 6 here]

[Place Figure 7 here]

[Place Figure 8 here]

FIGURE AND TABLE LEGENDS:

Table 1: Summary of criteria for infarct segmentation for different scan types.

Figure 1: Schematic illustration of the concept of voxel-based lesion-symptom mapping. The upper part shows the brain image pre-processing steps consisting of segmenting the lesion (an acute infarct in this case) followed by registration to a brain template (the MNI-152 template in this case). Below, a part of the registered binary lesion map of the same patient is shown as a 3D grid, where each cube represents a voxel. Taken together with the lesion maps of 99 other patients, a lesion overlay map is generated. For each voxel, a statistical test is performed to determine the association between lesion status and cognitive performance. The chi-squared test shown here is just an example, any statistical test could be used. Typically, hundreds of thousands of voxels are tested throughout the brain, followed by a correction for multiple comparisons.

Figure 2: Example of motion artifacts on a CT scan, presenting as shading, streaking and blurring in the image. Two different slices of a single CT scan are shown. Some examples of streaks and shades in the image are indicated by arrows. In this case, an infarct with a hemorrhagic component in the right cerebellar hemisphere is clearly visible, but a precise delineation of the lesion's anterior and medial border is difficult due to these artifacts. This scan should, therefore, not be used for LSM.

Figure 3: Segmentation and registration of an infarct on a CT scan. (A) CT scans at three timepoints for a single patient. The CT <24 h cannot be used for segmentation because the infarct is not yet visible even though the CT-perfusion maps shows ischemia in a large right frontal region. Legends to CT-perfusion maps: cerebral blood flow (CBF in mL/100 g/min) ranging 0 (dark blue) to 200 (red) and mean transit time (MTT in s) ranging from 0 (red) to dark blue (20). The CT scan on day 6 shows swelling of the infarcted brain tissue, with slight midline shift and hemorrhagic transformation visible as a region with higher density within the infarct. The CT scan after 4 months shows brain tissue loss with ex vacuo enlargement of ventricles and nearby sulci. The registration will have to compensate for the resulting displacement of adjacent structures. **(B)** Shown is the the result of registration to the MNI-152 template. The registration algorithm insufficiently compensated for the midline shift and compression of the left ventricle, which required a manual correction (shown on the right).

Figure 4: Examples of the fogging effect on CT imaging. Scans at three different timepoints are shown for two different patients to illustrate why a CT scan made in the fogging phase (i.e., 14-

21 days after stroke) should be avoided. (A) For patient 1, the CT scan performed 24 h after stroke onset shows a well-demarcated infarct in the left frontal lobe. 20 days after stroke onset, the infarct is not well-demarcated, and using this scan for segmentation would result in the underestimation of the infarct size. The follow-up MRI (3 years after) shows that the CT scan after 24 h was an accurate representation of the infarct size, whereas the CT scan at day 20 was not. (B) For patient 2, the CT scan within 24 h shows subtle early signs of ischemia with loss of gray-white matter differentiation and diffuse swelling in the right temporal and insular regions. The CT scan at day 4 shows a well-demarcated infarct. On the CT scan at day 18, a large part of the hypodense infarcted region has become isodense, which would result in undersegmentation of the infarct.

Figure 5: Segmentation and registration of an infarct on an MRI DWI sequence. MRI scan performed 12 h after stroke onset. (A) the acute ischemic lesion is hyperintense on the DWI sequence (b-value = 1000) and hypointense on the ADC, indicating restricted diffusion due to cytotoxic edema. The infarct is segmented on the DWI image. It should be noted that there is a subtle increase in signal on the FLAIR, but this is insufficiently clear to allow for lesion segmentation at this timepoint. (B) The dotted ellipse shows artifacts near bone-air configurations on the DWI (upper image) and ADC (lower image). (C) Comparison of the registered DWI sequence (left image; same scan as shown in panels A and B) and the corresponding registered infarct with the MNI-152 template (middle image). Note the slight error at the head of the right caudate nucleus, where the ventricles are not perfectly aligned. This required a manual correction of the segmentation in standard space (shown on the right).

Figure 6: Segmentation and registration of an infarct on an MRI FLAIR sequence. MRI scans were performed at two different timepoints after stroke for a single patient. (A) In the MRI scans for day 3 the acute lacunar infarct (indicated with white arrows) can be reliably distinguished from chronic hyperintense lesions, such as white matter hyperintensities (indicated with dashed circles), because only acute infarcts show diffusion restriction on the DWI. It should be noted that at this timepoint, the DWI can also be used for segmentation. (B) At 7 months, the DWI is no longer useful for distinguishing the infarct from white matter hyperintensities. Instead, the T1 should be used to identify the infarct based on the presence of a cerebrospinal fluid-filled cavity that has a low signal on T1 (and high signal on ADC). At this chronic stage, both the cavity and the surrounding hyperintense signal on FLAIR should be segmented as an infarct. (C) This shows the results of the registration of the FLAIR on day 3, which is adequate and requires no manual correction.

Figure 7: Overview of frequently used registration schemes implemented in RegLSM. The use of intermediate templates that provide a better match with the patient than the target template is optional. This is of particular importance when a CT scan is registered to an MRI template (see patient 1). When segmenting on FLAIR or DWI, the segmented scan can either be co-registered to a native T1 image (see patient 2), if available or directly registered to the T1 template (patient 3). Other alternatives are also available, as explained in the relevant sections of the discussion.

Figure 8: Registration result viewer implemented in RegLSM. The left three panels show the MNI-152 template in three planes (transversal, sagittal, coronal), and the right three panels show a registered DWI image in three planes. The crosshair helps can be used to verify if anatomical structures are accurately aligned.

Supplementary Figure 1: Typical folder structure during an image processing for LSM. The first subfolder for subject ID002 contains three native scans in nifti format (FLAIR, T1 and T2, in red box) and the segmentation of the FLAIR sequence (in blue box). The three subfolders are created during the registration process by RegLSM. The subfolder to_MNI contains the registered segmented scan (in this case the FLAIR, in green box). The subsequent subfolder contains the registered lesion map in standard space (purple box). Of note, RegLSM will be made BIDS-compatible in the upcoming update.

DISCUSSION:

LSM is a powerful tool to study the functional architecture of the human brain. A crucial step in any lesion-symptom mapping study is the preprocessing of imaging data, segmentation of the lesion and registration to a brain template. Here, we report a standardized pipeline for lesion segmentation and registration for the purpose of lesion-symptom mapping. This method can be performed with freely available image processing tools, can be used to process both CT and structural MRI scans, and covers the entire process of preparing the imaging data for lesion-symptom mapping analyses.

The first major step in processing brain imaging data for lesion-symptom mapping is lesion segmentation. This protocol provides a detailed tutorial including criteria for infarct delineation, several examples, and pitfalls to facilitate accurate and reproducible segmentation. As mentioned in the protocol and summarized in **Table 1**, each scan type has a specific time window in which it can be used for infarct segmentation. Infarcts are visible on DWI within several hours after stroke onset as hyperintense on DWI and hypointense on ADC (reflecting restricted water diffusion due to cytotoxic edema), whereas other MRI sequences, including FLAIR, (and CT scans) are not sensitive enough to reliably detect infarcts within 48 h³⁹. After the first week, the ADC image becomes isointense and eventually hyperintense as vasogenic edema develops³⁰, while the DWI usually remains hyperintense for several more weeks^{31,39,40}. It is therefore advised to use DWI only within 7 days and to use the FLAIR sequence after 7 days.

As noted in step 3.4, a FLAIR hyperintense lesion is not always an infarct. White matter hyperintensities and other chronic lesions can resemble a subcortical infarct on a FLAIR sequence. In the acute stage, small subcortical infarcts can easily be distinguished from white matter hyperintensities or other chronic lesions such as lacunes of presumed vascular origin when there is a DWI available, as mentioned in the protocol (see **Figure 5**). In the chronic stage, the T1 sequence needs be closely reviewed to look for small cavities (of at least 3 mm) within a lesion, indicating the lesion is not a white matter hyperintensity (see **Figure 6**). Cavities of <3 mm, particularly when elongated in shape, within a FLAIR hyperintense lesion are more likely to be a perivascular space than an infarct and are not to be segmented as infarcts³³. If a chronic cavitated lesion fits the criteria for a lacune (i.e., the cavity is 3–15 mm)³³, it can still be

challenging to ensure that this is in fact the symptomatic infarct, because lacunes can occur in individuals without overt neurological symptoms, and some individuals have multiple lacunes⁴¹. It helps to know the clinical stroke phenotype in these cases to ensure that the infarct is located in a structure that fits the initial stroke symptoms. When there is doubt whether a lacune corresponds with the stroke symptoms, it is best to exclude the patient.

There are several considerations regarding accurate infarct identification that need to be taken into account. The first concerns reliability of the scans in detecting brain infarcts. In minor ischemic stroke patients with small infarcts, final infarct size on follow-up FLAIR is often smaller than the initial DWI lesion⁴². In large (cortical) infarcts, there is considerable evidence that the DWI lesion in the hyperacute stage (<24 h) accurately represents the infarct core (i.e., represents irreversible damage), even when DWI imaging is performed before the reperfusion therapy^{43,44}. However, in some cases, the DWI lesion seen within 24 h is an underrepresentation of the final infarct size, because the penumbra (hypoperfused but potentially salvageable brain tissue) is not visible as a DWI lesion, but it may still progress to form part of the final infarct⁴³ (particularly if reperfusion therapy is not performed in patients with large artery occlusions).

Another issue with using DWI within 24 h is that DWI lesions are to some extent dynamic and may show reversal after reperfusion therapy. However, follow-up scans showed that this reversal was transient and that the initial DWI lesion did accurately represent the infarct core. However, this does indicate that DWI performed several hours after reperfusion therapy might result in further underestimation of the final infarct size⁴³. This potential underestimation of the final infarct size is an important limitation of using DWI performed within 24 h after stroke onset in lesion-symptom mapping studies. However, it should be noted that there are limitations to using other scan protocols as well. First of all, scans of any modality that are performed >24 h after the stroke can show mass effect due to swelling of the infarct in the acute stage, and ex vacuo enlargement of ventricles, sulcal widening, and displacement of surrounding structures in the chronic stage⁷. This displacement should be corrected by the registration algorithm and, if necessary, a manual correction should be performed by an expert reviewer. Still, both conditions can affect the accuracy of the translation of the infarcted region to standard space, even when rigorous quality checks are performed.

Of note, DWI in the hyperacute stage does not suffer from this limitation, since there is no significant mass effect within 24 h. In light of these scanner type-specific limitations, consideration of obtaining a homogeneous dataset should be made when designing a lesion-symptom mapping study, using a single scan type at a standardized timepoint. However, this will introduce a systematic bias in patient inclusion, as in most clinics, stroke patients that undergo MRI are different (i.e., often have smaller infarcts and less, more isolated symptoms) compared to patients that undergo CT. As such, systematically excluding patients with a specific imaging modality will limit the variability in lesion distribution, which in turn has a negative impact on the validity of the lesion-symptom mapping results⁴⁵.

Finally, a limitation of all structural imaging modalities is that they do not capture the presence

of decreased perfusion around the infarct, even though abnormal perfusion in brain regions that appear normal on structural imaging can interfere with brain function^{7,46}. In summary, CT and several structural MRI sequences can be used to segment infarcts for the purpose of lesion-symptom mapping, as long as the proper time windows and criteria for lesion detection are followed, and the registration results are carefully checked. Taking into account scanner type-specific and time window-specific limitations is crucial when designing and interpreting lesion-symptom mapping studies.

An important issue in any lesion segmentation method is evaluating its reproducibility. Adequate training and knowledge of brain anatomy are crucial to distinguish lesions from normal anatomical structures and anatomical variants. Also, evaluation of inter- and intra-observer reproducibility prior to performing infarct segmentations for the purpose of lesion-symptom mapping is recommended. We have previously demonstrated high inter-observer agreement for the manual infarct segmentation protocol on CT scans in both the acute [mean Dice Similarity Coefficient (DSC) 0.77; SD 0.11] and chronic (DSC 0.76; SD 0.16) stages, as well as high intra-observer agreement (DSC 0.90, SD 0.05 in acute stage; DSC 0.89, SD 0.06 in chronic stage)¹⁶. The inter-observer agreement for infarct segmentation on DWI and FLAIR is also known to be high⁴⁷.

The main limitation of the method described here is that manual segmentation, quality checks, and manual corrections are time-consuming. Fully automated infarct segmentation tools that can process both CT and MRI scans with varying scan protocols in a reliable manner are lacking^{7,47}. Automated infarct segmentation tools that are optimized for specific scan protocols do provide promising results (e.g., for DWI where the contrast between infarcted and normal brain tissue is very high⁴⁸), and further improvements are likely to be made in the near future. Semi-automated methods can reduce the time needed for segmenting infarcts but also require an expert to ensure accurate lesion classification⁴⁷. This quality check is crucial, because even a few failed infarct segmentations may significantly reduce the validity of the lesion-symptom mapping results. Thus, manual infarct segmentation remains the gold standard⁷.

The second major step in processing brain imaging data for lesion-symptom mapping is the registration of the lesion maps to a brain template. RegLSM provides multiple validated registration schemes. For CT scans, histogram equalization is performed to improve soft-tissue contrast²¹, and an intermediate registration step to a CT template²² is performed to optimize the registration quality. For MRI scans, the scan on which the segmentation was performed is co-registered to the corresponding T1 sequence, if available, using linear registration. Subsequently, the native T1 is registered to an intermediate age-specific T1 template²² or directly to the target T1 template³⁴ using linear and non-linear registration²⁰. The intermediate templates, both CT and T1, have been aligned with the target T1 template using a linear and non-linear registration that was manually optimized and verified. When the intermediate template is used, this pre-computed transformation is appended as the final transformation step.

When no T1 is available, the scan on which the segmentation was performed (usually a FLAIR or

DWI) can be registered directly to the target T1 template using a linear and non-linear registration²⁰. For DWI images, a brain tissue mask is created using unified segmentation as implemented in SPM³⁵, to guide the linear registration after with a non-linear registration completes the procedure. The registration schemes in RegLSM are highly customizable, and the commonly used MNI-152 T1 template and intermediate template can be replaced by any template that may provide a better match with the segmented scan. An interesting possibility would be the development of FLAIR and DWI brain templates that provide a better match with individual stroke patients. A limitation of the described registration method is that the registration fails in some cases, meaning a visual inspection of the registration results is required for all patients, followed by a manual correction in some cases. The number of cases that require a manual correction varies with stroke subtype. In our previous experience, manual corrections are needed in up to one-third of large brain infarcts⁴⁹⁻⁵¹ but only 13% of patients with small lacunar infarcts⁴. The majority of failed registrations is caused by anatomical distortions due to the lesion (as discussed previously), which is particularly likely to happen in cases of large infarcts with either severe swelling or ex vacuo enlargement of surrounding structures. The manual correction of these misalignments is time-consuming but crucial before performing lesion-symptom mapping analyses. The number of cases that require manual correction is lower when studying white matter hyperintensities compared to infarcts, probably because these lesions do not cause significant anatomical distortion. In our recent lesion-symptom mapping study in patients with white matter hyperintensities, only 3% were of insufficient quality to proceed without manual correction⁶.

By default, RegLSM does not apply any form of lesion masking nor lesion filling, although the customizable nature of RegLSM allows users to enable it. The use of mutual information metric⁵² in the registration procedure avoids most of the issues previously raised with the presence of a lesion affecting the registration quality. Mutual information is well-suited for multi-modal registrations (e.g., FLAIR to T1) and is less affected by the presence of pathology than other metrics or cost-functions. Even for intra-modal registration (e.g., the subject T1 to the template T1), mutual information should be used to cope with the presence of pathology. Lesions will have their own cluster in the joint histogram that can be optimized without affecting registration quality. In some cases, lesion masking can even degrade the registration quality, since insufficient image information remains to guide the registration when the lesion volume is large.

As a general comment regarding the software used, including conversion from DICOM to nifti format, scan visualization, and annotation, it should be noted that many open-access tools exist. We did not provide a systematic overview of all the available tools, because this was beyond the scope of this article. Also, many institutions develop their own image visualization and annotation tools. Here, we chose to provide a comprehensive framework that covers the entire process of CT/MRI preprocessing, segmentation, and registration for the purpose of lesion-symptom mapping using several commonly used open-access tools. When using this method, the proposed image conversion, visualization, or annotation tools could be replaced by other available tools or by custom-made tools, if this better suits the data or is considered more convenient. Also, the image processing pipeline can be further customized by implementing

available (semi-)automated infarct segmented tools, if this fits the study design of a particular lesion-symptom mapping study. This paper focuses on processing scans of patients with ischemic stroke, but the framework can be used for processing other lesion types as well (e.g., white matter hyperintensities or lacunes) by replacing the lesion segmentation procedure (section 3 of the protocol) with another appropriate segmentation procedure.

An important issue in lesion-symptom mapping is how to deal with co-occurring pathologies. For example, when performing a study in patients with acute ischemic stroke, there may be a substantial amount of co-occurring white matter hyperintensities or even previous infarcts. When studying white matter hyperintensities, some patients may also have (silent or clinically overt) brain infarcts. Co-occurring pathologies on brain imaging can have an independent contribution to cognitive impairment and should ideally be taken into account. A straightforward way of dealing with this issue is to exclude patients with co-occurring pathologies [e.g., exclude patients with (large) brain infarcts when focusing on white matter hyperintensities], but this has the disadvantage of limiting the generalizability of the findings to patients with a single type of pathology.

An alternative approach that is often used is regressing out the effects of co-occurring pathologies (e.g., adjust for white matter hyperintensity volume or the presence of brain infarcts) on the outcome variable prior to or during the lesion-symptom mapping analysis. However, a limitation of this approach is that the location of these co-occurring pathologies is not taken into account, even though this is known to be relevant for infarcts and white matter hyperintensities², and likely for other lesion types. Therefore, on theoretical grounds, the best approach is to perform an integrated lesion-symptom mapping analysis in which the VLSM results are corrected for the location of co-occurring pathologies at the voxel-level. In a recent study, a multivariate support vector regression-based method was used to perform integrated voxel-wise lesion-symptom mapping on multiple lesion types and identified brain regions where white matter hyperintensities are associated with cognitive decline after stroke, independent of acute infarct location⁵³. This study shows how an integrated voxel-wise analysis of multiple lesion types can provide new insights into the complex interaction between different lesion types in the development of cognitive impairment and dementia⁵³.

In summary, the image processing pipeline provided here serves as a standardized method of brain lesion segmentation and registration for the purpose of lesion-symptom mapping. The strengths of this method are the (1) reliability of the segmentation and registration method, which comes at the cost of rigorous quality checks, and in some cases corrections by a trained rater, (2) customizability of the registration pipeline in which the registration scheme and templates can be adjusted to fit the data in the best possible way, and (3) possibility to process highly heterogeneous brain imaging data, including CT and structural MRI sequences. Future challenges include the development of robust, automated lesion segmentation tools for CT and MRI, further improvements of the registration methods, and development of brain templates that provide a better match with individual stroke patients, including DWI and FLAIR templates. These improvements may further increase the reproducibility of lesion segmentation and reduce the time spent on performing visual checks and manual corrections.

ACKNOWLEDGMENTS:

The work of Dr. Biesbroek is supported by a Young Talent Fellowship from the Brain Center Rudolf Magnus of the University Medical Center Utrecht. This work and the Meta VCI Map consortium are supported by Vici Grant 918.16.616 from ZonMw, The Netherlands, Organisation for Health Research and Development, to Geert Jan Biessels. The authors would like to thank Dr. Tanja C.W. Nijboer for sharing scans that were used in one of the figures.

DISCLOSURES:

The authors disclose no conflicts of interest.

REFERENCES:

1. Rorden, C., Karnath, H.O. Using human brain lesions to infer function: A relic from a past era in the fMRI age? *Nature Reviews Neuroscience*. **5** (10), 812–819, doi: 10.1038/nrn1521 (2004).
2. Biesbroek, J.M., Weaver, N.A., Biessels, G.J. Lesion location and cognitive impact of cerebral small vessel disease. *Clinical Science (London, England: 1979)*. **131** (8), 715–728, doi: 10.1042/CS20160452 (2017).
3. Karnath, H.O., Sperber, C., Rorden, C. Mapping human brain lesions and their functional consequences. *NeuroImage*. **165**, 180–189, doi: 10.1016/j.neuroimage.2017.10.028 (2018).
4. Zhao, L. et al. Strategic infarct location for post-stroke cognitive impairment: A multivariate lesion-symptom mapping study. *Journal of Cerebral Blood Flow and Metabolism : An Official Journal of the International Society of Cerebral Blood Flow and Metabolism*. **38** (8), 1299–1311, doi: 10.1177/0271678X17728162 (2018).
5. Weaver, N. A. et al. The Meta VCI Map consortium for meta-analyses on strategic lesion locations for vascular cognitive impairment using lesion-symptom mapping: design and multicenter pilot study. *Alzheimer's and Dementia: Diagnosis, Assessment and Disease Monitoring*.
6. Biesbroek, J. M. et al. Impact of Strategically Located White Matter Hyperintensities on Cognition in Memory Clinic Patients with Small Vessel Disease. *PLoS One*. **11** (11), e0166261, doi: 10.1371/journal.pone.0166261 (2016).
7. de Haan, B., Karnath, H. O. A hitchhiker's guide to lesion-behaviour mapping. *Neuropsychologia*. **115**, 5–16, doi: 10.1016/j.neuropsychologia.2017.10.021 (2018).
8. Duering, M. et al. Strategic role of frontal white matter tracts in vascular cognitive impairment: A voxel-based lesion-symptom mapping study in CADASIL. *Brain*. **134**, (Pt8), 2366–2375, doi: 10.1093/brain/awr169 (2011).
9. Biesbroek, J. M. et al. Association between subcortical vascular lesion location and cognition: a voxel-based and tract-based lesion-symptom mapping study. The SMART-MR study. *PLoS One*. **8** (4), e60541, doi: 10.1371/journal.pone.0060541 (2013).
10. Wu, O. et al. Role of Acute Lesion Topography in Initial Ischemic Stroke Severity and Long-Term Functional Outcomes. *Stroke*. **46** (9), 2438–2444, doi: 10.1161/STROKEAHA.115.009643 (2015).

- 881 11. Mah, Y. H., Husain, M., Rees, G., Nachev, P. Human brain lesion-deficit inference
882 remapped. *Brain*. **137** (Pt8) 2522-2531, doi: 10.1093/brain/awu164 (2014).
- 883 12. Sperber, C., Karnath, H. O. Impact of correction factors in human brain lesion-behavior
884 inference. *Human Brain Mapping*. **38** (3), 1692-1701, doi: 10.1002/hbm.23490 (2017).
- 885 13. Chen, R., Herskovits, E. H. Voxel-based Bayesian lesion-symptom mapping. *NeuroImage*.
886 **49** (1), 597-602, doi: 10.1016/j.neuroimage.2009.07.061 (2010).
- 887 14. Y., Z., D. Y., K., H. B., C., M. F., S., Z., W. Multivariate lesion-symptom mapping using
888 support vector regression. *Human Brain Mapping*. **35** (12), 5861–5876, doi:
889 10.1002/hbm.22590 (2014).
- 890 15. Corbetta, M. et al. Common behavioral clusters and subcortical anatomy in stroke.
891 *Neuron*. **85** (5), 927-941, doi: 10.1016/j.neuron.2015.02.027 (2015).
- 892 16. Biesbroek, J. M. et al. The anatomy of visuospatial construction revealed by lesion-
893 symptom mapping. *Neuropsychologia*. **62**, 68–76, doi:
894 10.1016/j.neuropsychologia.2014.07.013 (2014).
- 895 17. Duering, M. et al. Strategic white matter tracts for processing speed deficits in age-
896 related small vessel disease. *Neurology*. **82** (22), 1946-1950, doi:
897 10.1212/WNL.0000000000000475 (2014).
- 898 18. Yourganov, G., Fridriksson, J., Rorden, C., Gleichgerrcht, E., Bonilha, L. Multivariate
899 Connectome-Based Symptom Mapping in Post-Stroke Patients: Networks Supporting
900 Language and Speech. *The Journal of Neuroscience*. **36** (25), 6668-6679, doi:
901 10.1523/JNEUROSCI.4396-15.2016 (2016).
- 902 19. Zavaglia, M., Forkert, N. D., Cheng, B., Gerloff, C., Thomalla, G., Hilgetag, C. C. Mapping
903 causal functional contributions derived from the clinical assessment of brain damage
904 after stroke. *NeuroImage: Clinical*. **9**, 83-94, doi: 10.1016/j.nicl.2015.07.009 (2015).
- 905 20. Klein, S., Staring, M., Murphy, K., Viergever, M. A., Pluim, J. P. W. Elastix: A toolbox for
906 intensity-based medical image registration. *IEEE Transactions on Medical Imaging*. **29** (1),
907 196-205, doi: 10.1109/TMI.2009.2035616 (2010).
- 908 21. Kuijf, H. J., Biesbroek, J. M., Viergever, M. A., Biessels, G. J., Vincken, K. L. Registration of
909 brain CT images to an MRI template for the purpose of lesion-symptom mapping. *Lecture*
910 *Notes in Computer Science (including subseries Lecture Notes in Artificial Intelligence and*
911 *Lecture Notes in Bioinformatics)*. doi: 10.1007/978-3-319-02126-3_12 (2013).
- 912 22. Rorden, C., Bonilha, L., Fridriksson, J., Bender, B., Karnath, H. O. Age-specific CT and MRI
913 templates for spatial normalization. *NeuroImage*. **61** (4), 957-965, doi:
914 10.1016/j.neuroimage.2012.03.020 (2012).
- 915 23. Barrett, J. F., Keat, N. Artifacts in CT: Recognition and Avoidance. *RadioGraphics*. doi:
916 10.1148/rg.246045065 (2007).
- 917 24. Zhuo, J., Gullapalli, R. P. AAPM/RSNA physics tutorial for residents: MR artifacts, safety,
918 and quality control. *Radiographics: a review publication of the Radiological Society of*
919 *North America, Inc.* doi: 10.1148/rg.261055134 (2007).
- 920 25. Rorden, C., Brett, M. Stereotaxic display of brain lesions. *Behavioural Neurology*. **12** (4),
921 191-200, doi: 10.1155/2000/421719 (2000).
- 922 26. Gorgolewski, K. J. et al. The brain imaging data structure, a format for organizing and
923 describing outputs of neuroimaging experiments. *Scientific Data*. **3**, 160044, doi:
924 10.1038/sdata.2016.44 (2016).

- 925 27. Yushkevich, P. A. et al. User-guided 3D active contour segmentation of anatomical
926 structures: Significantly improved efficiency and reliability. *NeuroImage*. **31** (3), 1116-
927 1128, doi: 10.1016/j.neuroimage.2006.01.015 (2006).
- 928 28. Becker, H., Desch, H., Hacker, H., Pencz, a CT fogging effect with ischemic cerebral
929 infarcts. *Neuroradiology*. **18** (4), 185-192, doi: 10.1007/BF00345723 (1979).
- 930 29. Kingsley, P. B., Monahan, W. G. Selection of the Optimum b Factor for Diffusion-
931 Weighted Magnetic Resonance Imaging Assessment of Ischemic Stroke. *Magnetic*
932 *Resonance in Medicine*. **51**, 996-1001, doi: 10.1002/mrm.20059 (2004).
- 933 30. Shen, J. M., Xia, X. W., Kang, W. G., Yuan, J. J., Sheng, L. The use of MRI apparent
934 diffusion coefficient (ADC) in monitoring the development of brain infarction. *BMC*
935 *Medical Imaging*. **11** (2) doi: 10.1186/1471-2342-11-2 (2011).
- 936 31. Lansberg, M. G. et al. Evolution of apparent diffusion coefficient, diffusion-weighted,
937 and T2-weighted signal intensity of acute stroke. *American Journal of Neuroradiology*. **22**
938 (4), 637-644 (2001).
- 939 32. Geijer, B., Sundgren, P.C., Lindgren, A., Brockstedt, S., Ståhlberg, F., Holtås, S. The value
940 of b required to avoid T2 shine-through from old lacunar infarcts in diffusion-weighted
941 imaging. *Neuroradiology*. **43** (7), 511-517, doi: 10.1007/s002340100544 (2001).
- 942 33. Wardlaw, J. M. et al. Neuroimaging standards for research into small vessel disease and
943 its contribution to ageing and neurodegeneration. *The Lancet Neurology*. **12** (8), 822-838,
944 doi: 10.1016/S1474-4422(13)70124-8 (2013).
- 945 34. Fonov, V., Evans, A. C., Botteron, K., Almli, C. R., McKinstry, R. C., Collins, D. L. Unbiased
946 average age-appropriate atlases for pediatric studies. *NeuroImage*. **54** (1), 313-327, doi:
947 10.1016/j.neuroimage.2010.07.033 (2011).
- 948 35. Ashburner, J., Friston, K. J. Unified segmentation. *NeuroImage*. **26** (3), 839-851, doi:
949 10.1016/j.neuroimage.2005.02.018 (2005).
- 950 36. Desikan, R. S. et al. An automated labeling system for subdividing the human cerebral
951 cortex on MRI scans into gyral based regions of interest. *NeuroImage*. **31** (3), 968-980,
952 doi: 10.1016/j.neuroimage.2006.01.021 (2006).
- 953 37. Hua, K. et al. Tract probability maps in stereotaxic spaces: Analyses of white matter
954 anatomy and tract-specific quantification. *NeuroImage*. **39** (1), 336-347, doi:
955 10.1016/j.neuroimage.2007.07.053 (2008).
- 956 38. Eickhoff, S. B. et al. A new SPM toolbox for combining probabilistic cytoarchitectonic
957 maps and functional imaging data. *NeuroImage*. **25** (4), 1325-1335, doi:
958 10.1016/j.neuroimage.2004.12.034 (2005).
- 959 39. Ricci, P. E., Burdette, J. H., Elster, A. D., Reboussin, D. M. A comparison of fast spin-echo,
960 fluid-attenuated inversion-recovery, and diffusion-weighted MR imaging in the first 10
961 days after cerebral infarction. *American Journal of Neuroradiology*. **20** (8), 1535-1542,
962 doi: 10.1121/1.398490 (1999).
- 963 40. Eastwood, J. D., Engelter, S. T., MacFall, J. F., Delong, D. M., Provenzale, J. M.
964 Quantitative assessment of the time course of infarct signal intensity on diffusion-
965 weighted images. *American Journal of Neuroradiology*. **24** (4), 680-687, (2003).
- 966 41. Wardlaw, J. M. What is a lacune? *Stroke*. **39**, 2921-2922, doi:
967 10.1161/STROKEAHA.108.523795 (2008).
- 968 42. Kate, M. P. et al. Dynamic Evolution of Diffusion-Weighted Imaging Lesions in Patients

969 With Minor Ischemic Stroke. *Stroke: a Journal of Cerebral Circulation*. **46**, 2318-2341, doi:
970 10.1161/STROKEAHA.115.009775 (2015).

- 971 43. Inoue, M. et al. Early diffusion-weighted imaging reversal after endovascular reperfusion
972 is typically transient in patients imaged 3 to 6 hours after onset. *Stroke*. **45**, 1024-1028,
973 doi: 10.1161/STROKEAHA.113.002135 (2014).
- 974 44. Campbell, B. C. V. et al. The infarct core is well represented by the acute diffusion lesion:
975 Sustained reversal is infrequent. *Journal of Cerebral Blood Flow and Metabolism*. **32** (1),
976 doi: 10.1038/jcbfm.2011.102 (2012).
- 977 45. Sperber, C., Karnath, H. O. On the validity of lesion-behaviour mapping methods.
978 *Neuropsychologia*. **115**, 17-24, doi: 10.1016/j.neuropsychologia.2017.07.035 (2018).
- 979 46. Hillis, A. E. et al. Restoring Cerebral Blood Flow Reveals Neural Regions Critical for
980 Naming. *Journal of Neuroscience*. **26** (31), 8069-8073, doi: 10.1523/JNEUROSCI.2088-
981 06.2006 (2006).
- 982 47. Wilke, M., de Haan, B., Juenger, H., Karnath, H. O. Manual, semi-automated, and
983 automated delineation of chronic brain lesions: A comparison of methods. *NeuroImage*.
984 **56** (4), 2038-2046, doi: 10.1016/j.neuroimage.2011.04.014 (2011).
- 985 48. Zhang, R. et al. Automatic Segmentation of Acute Ischemic Stroke From DWI Using 3-D
986 Fully Convolutional DenseNets. *IEEE Transactions on Medical Imaging*. **37** (9), 2149-2160,
987 doi: 10.1109/TMI.2018.2821244 (2018).
- 988 49. Biesbroek, J. M. et al. Distinct anatomical correlates of discriminability and criterion
989 setting in verbal recognition memory revealed by lesion-symptom mapping. *Human*
990 *Brain Mapping*. **36** (4), 1292–1303, doi: 10.1002/hbm.22702 (2015).
- 991 50. Biesbroek, J. M., van Zandvoort, M. J. E., Kappelle, L. J., Velthuis, B. K., Biessels, G. J.,
992 Postma, A. Shared and distinct anatomical correlates of semantic and phonemic fluency
993 revealed by lesion-symptom mapping in patients with ischemic stroke. *Brain Structure &*
994 *Function*. **221** (4), 2123–2134, doi: 10.1007/s00429-015-1033-8 (2016).
- 995 51. Ten Brink, A. F. et al. The right hemisphere is dominant in organization of visual search-A
996 study in stroke patients. *Behavioural Brain Research*. **304**, 71–79, doi:
997 10.1016/j.bbr.2016.02.004 (2016).
- 998 52. Pluim, J. P. W., Maintz, J. B. A. A., Viergever, M. A. Mutual-information-based registration
999 of medical images: A survey. *IEEE Transactions on Medical Imaging*. **22** (8), 986–1004,
1000 doi: 10.1109/TMI.2003.815867 (2003).
- 1001 53. Zhao, L. et al. The additional contribution of white matter hyperintensity location to
1002 post-stroke cognitive impairment: Insights from a multiple-lesion symptom mapping
1003 study. *Frontiers in Neuroscience*. **12** (MAY), doi: 10.3389/fnins.2018.00290 (2018).
- 1004

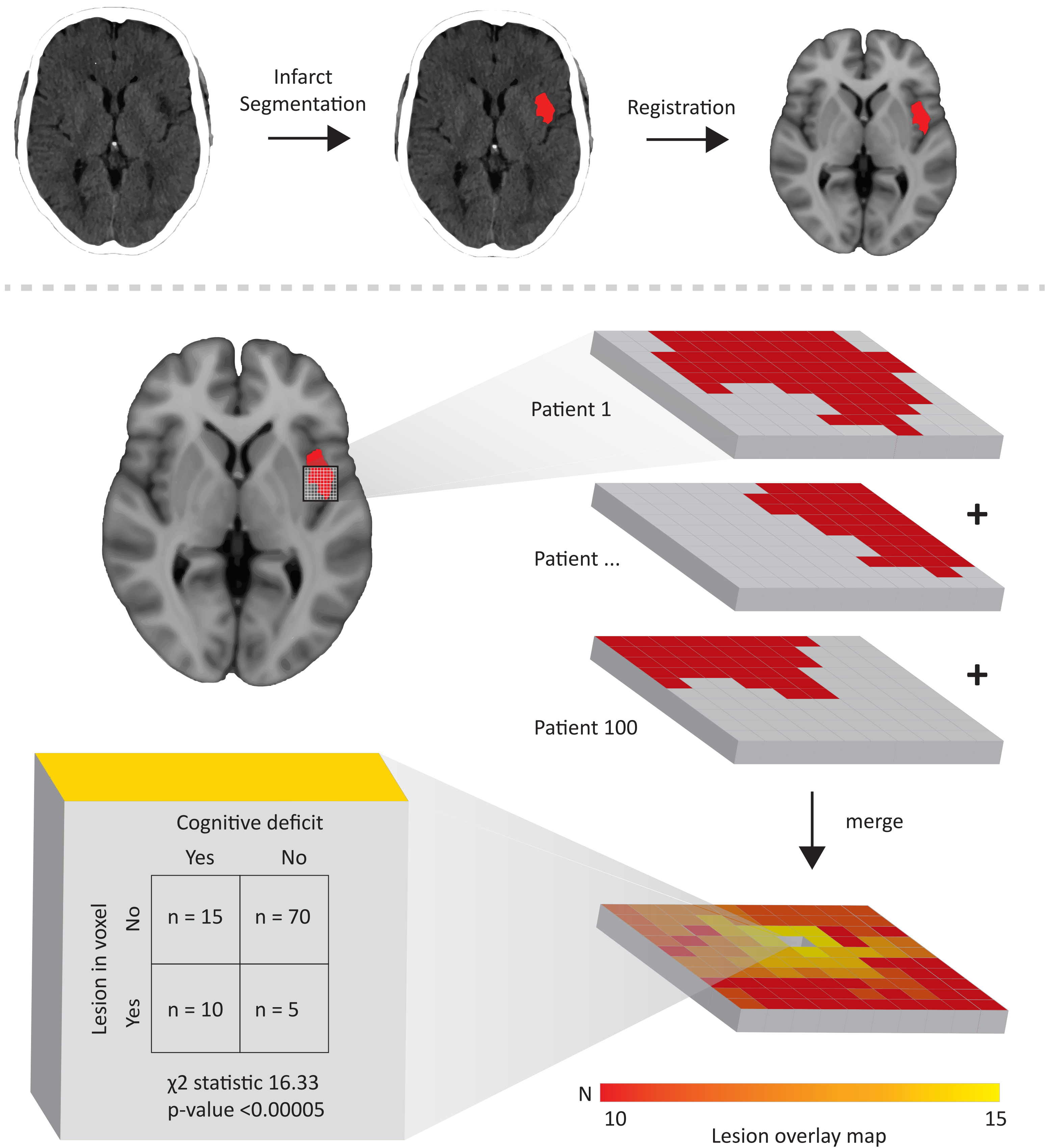
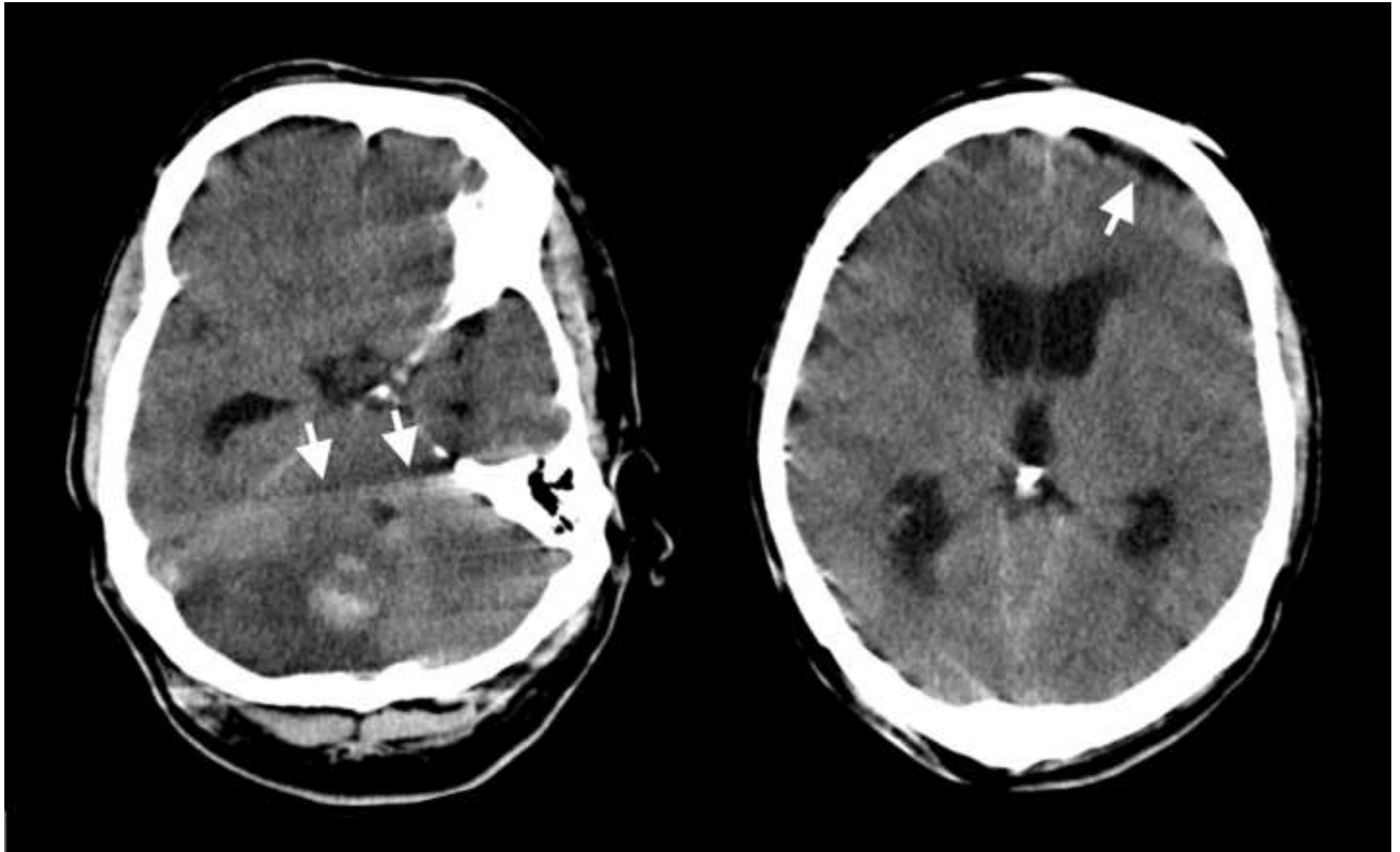
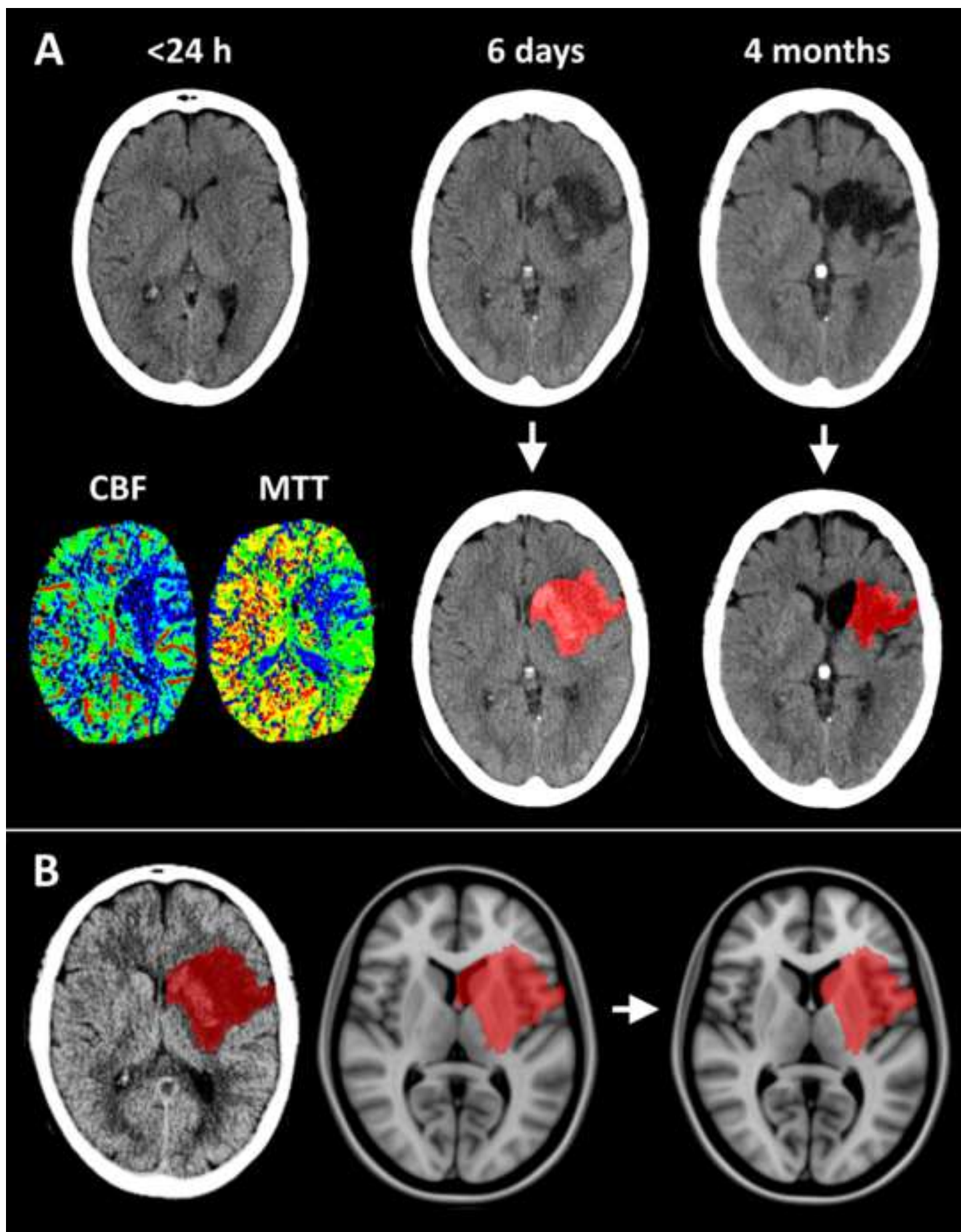
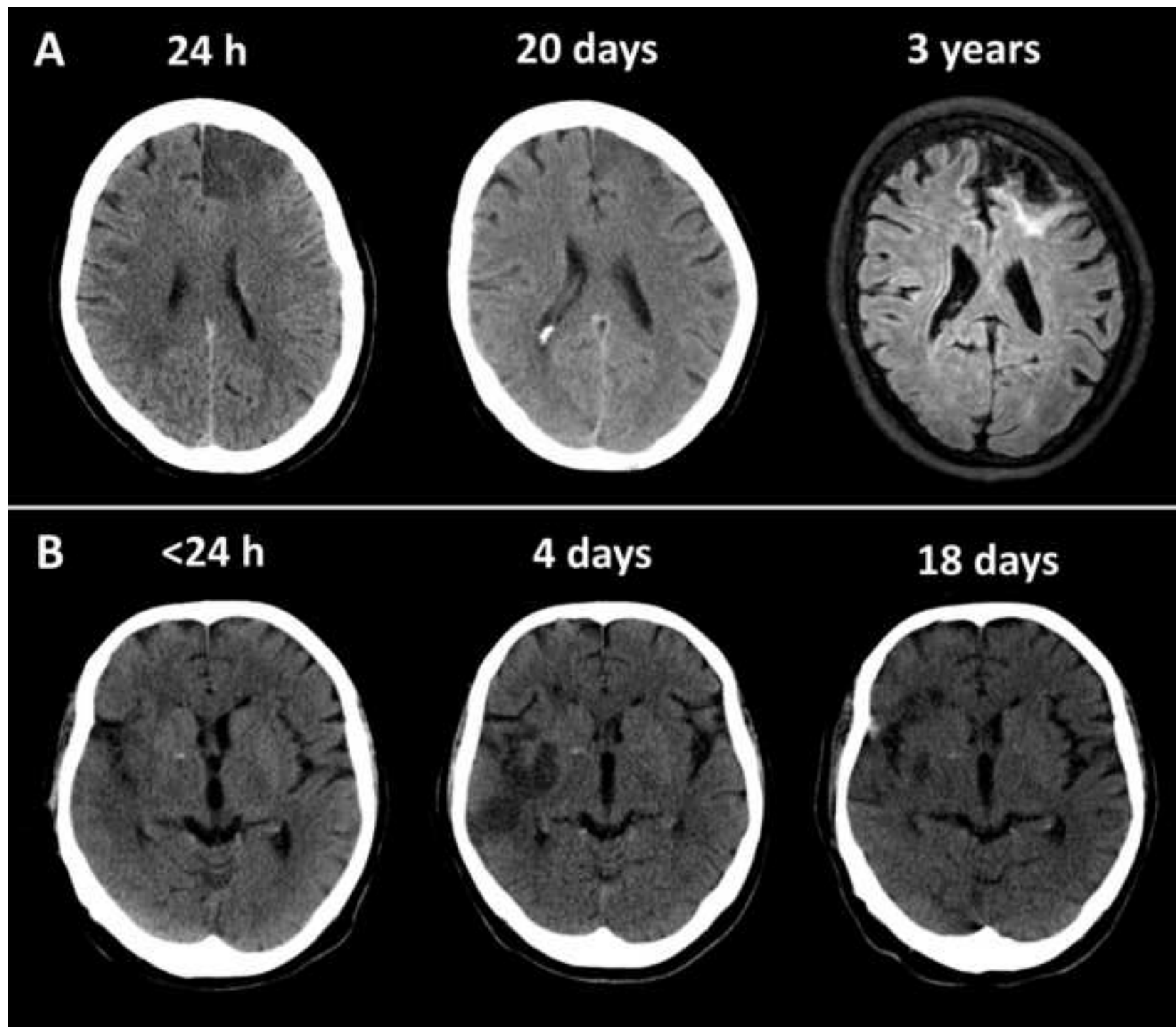


Figure 2

[Click here to access/download;Figure;Figure 2.tif](#)







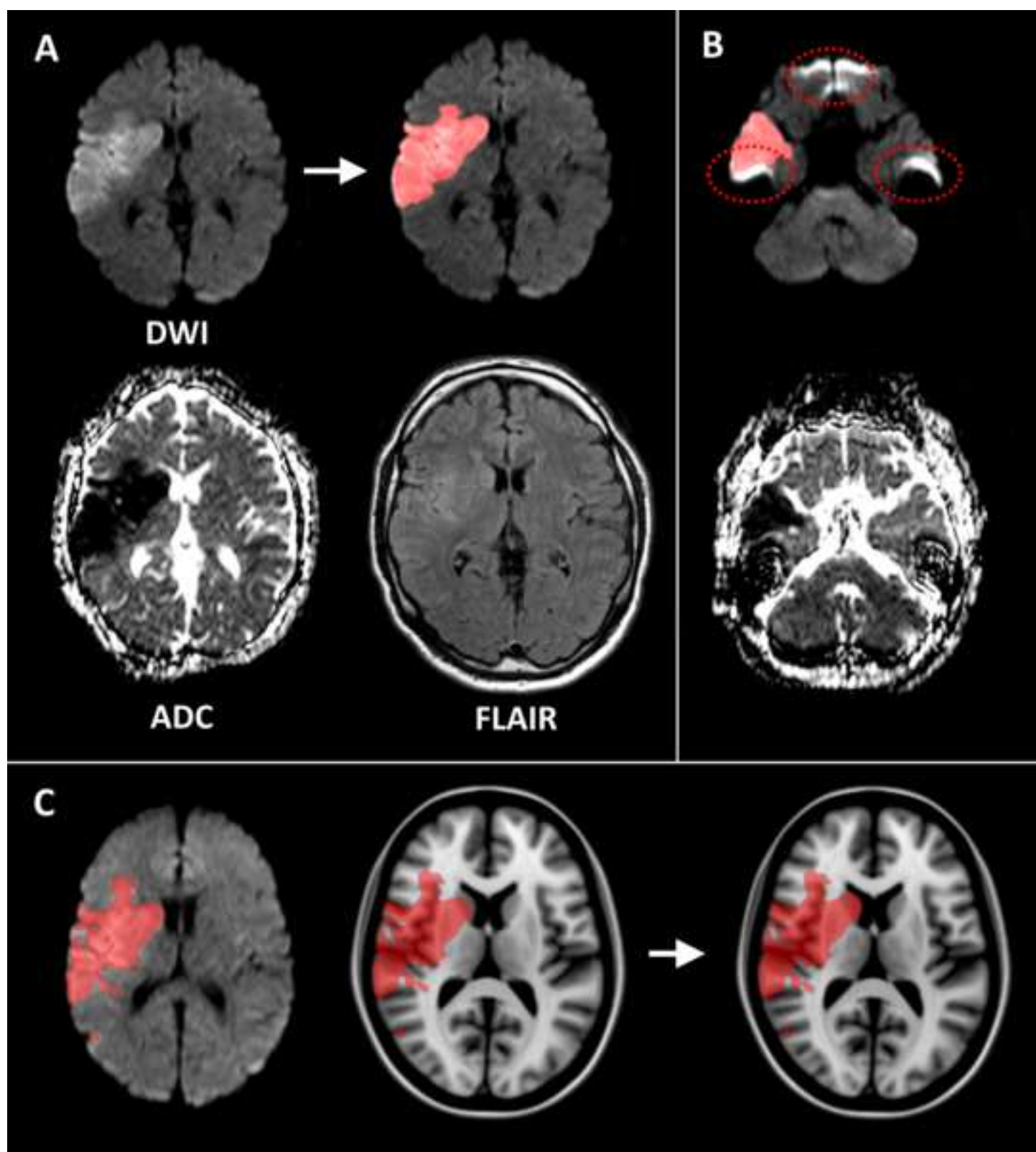


Figure 6

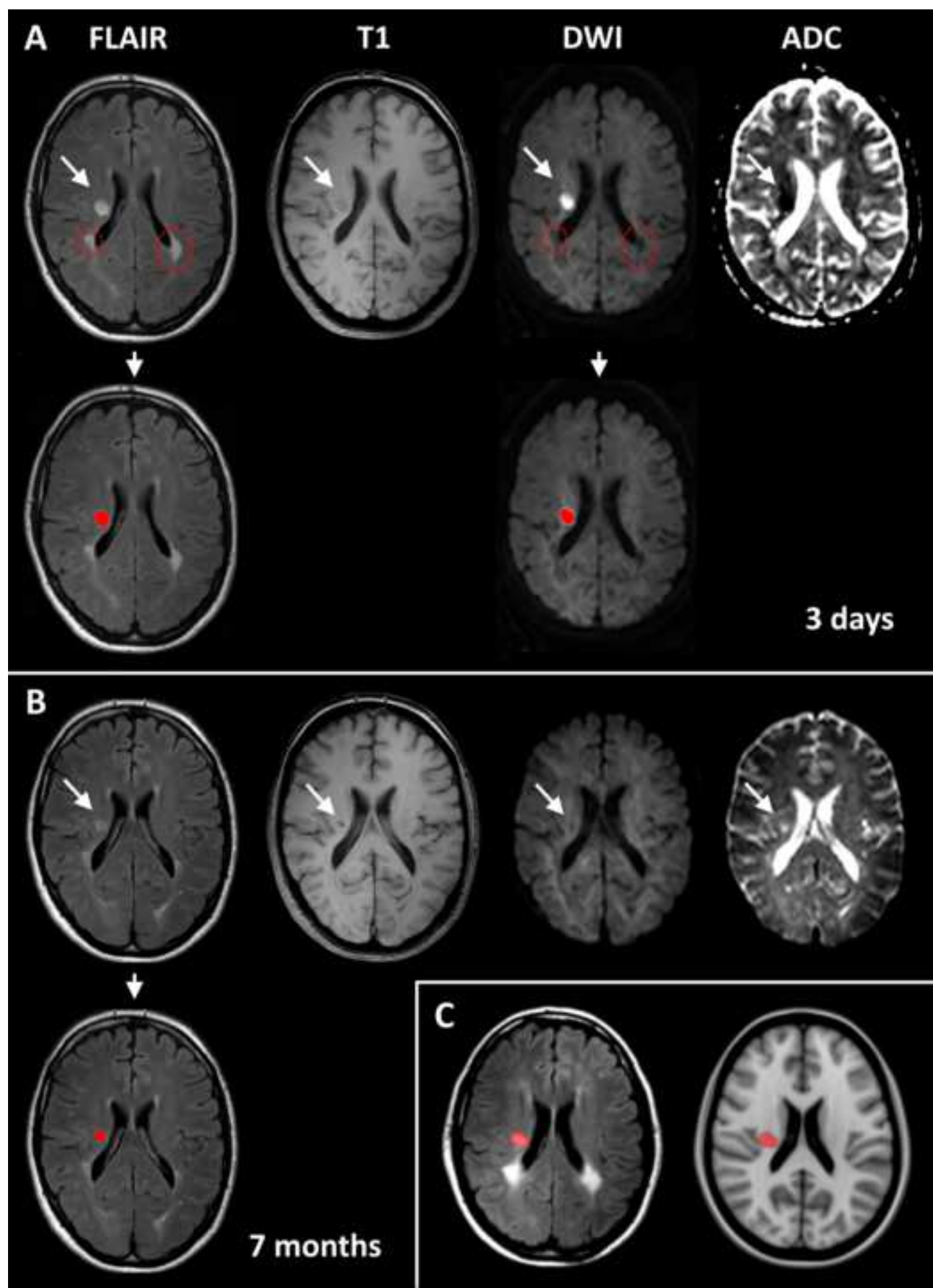


Figure 7

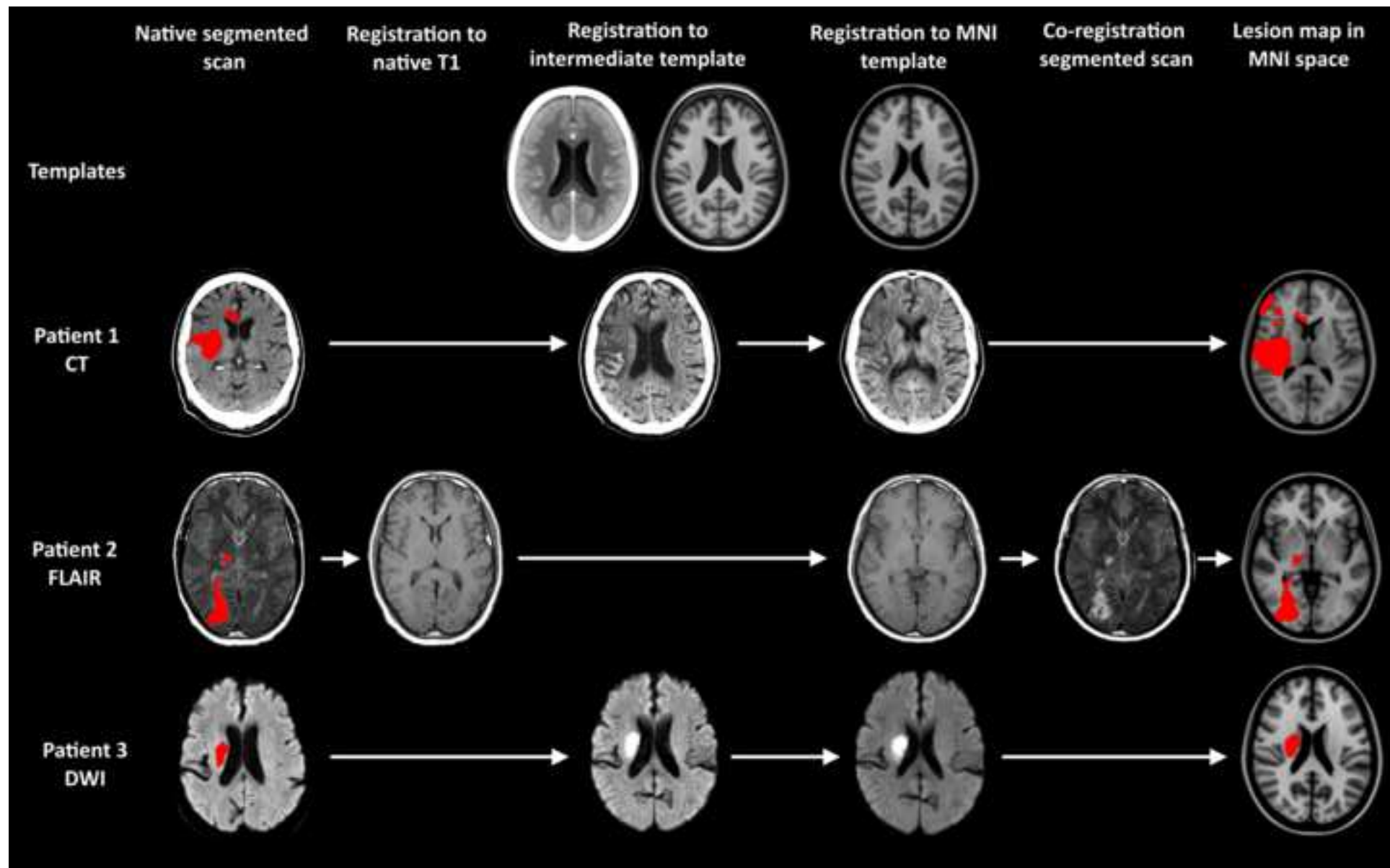
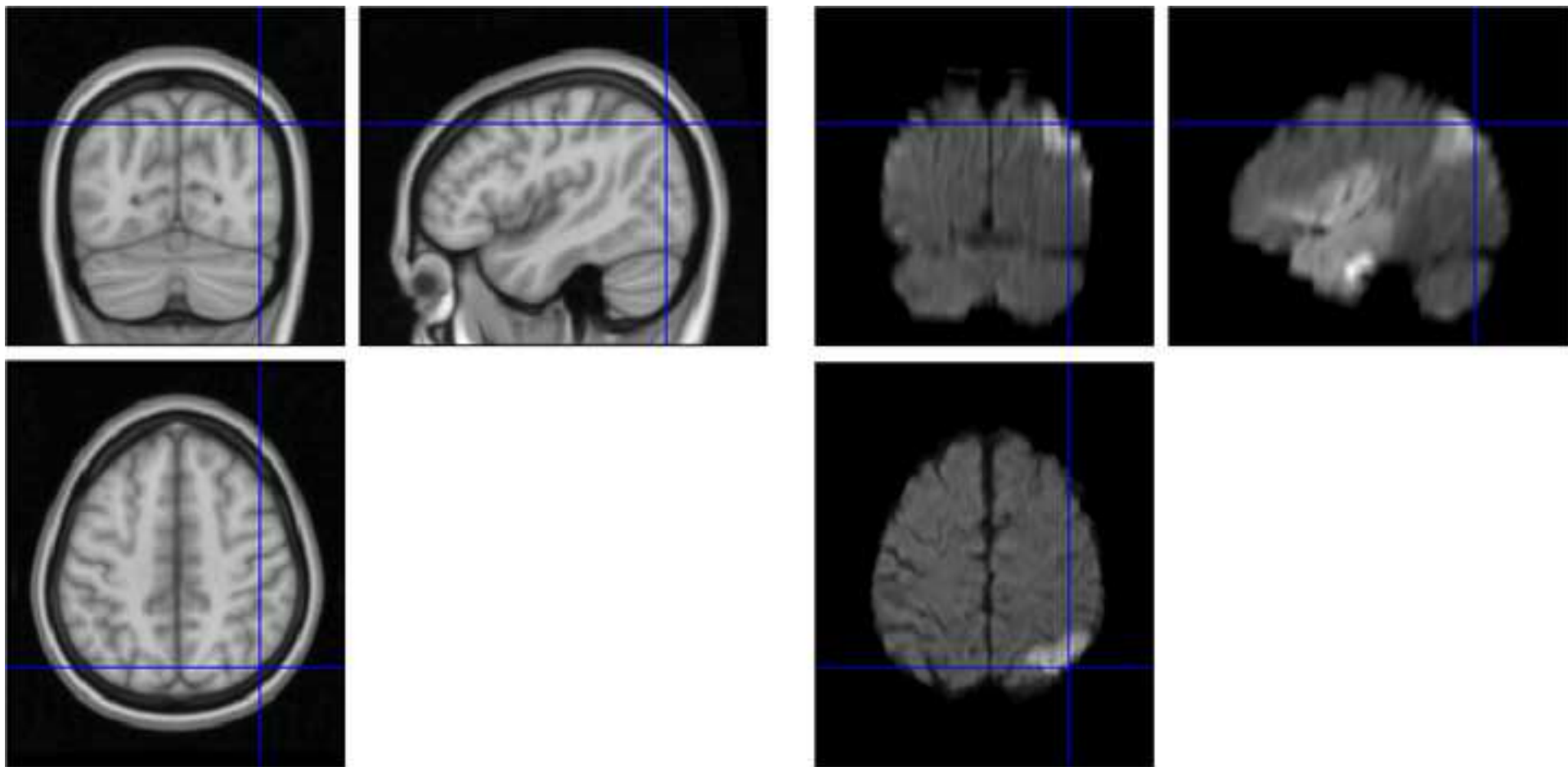


Figure 8

[Click here to access/download;Figure;Figure 8.tif](#)



Scan type	Time window after stroke	Infarct properties
CT	> 24 hours	Acute: hypodense Chronic: hypodense cavity with CSF and less hypodense rim
DWI	< 7 days	Hyperintense
FLAIR	> 48 hours	Acute: hyperintense Chronic: hypointense or isointense (cavity), hyperintense rim

Reference scan	Pitfalls
-	<ul style="list-style-type: none"> - Fogging phase - hemorrhagic transformation
ADC: typically hypointense	<ul style="list-style-type: none"> - T2 shinethrough - High DWI signal near interfaces between air and bone/tissue
<p>Acute: DWI/ADC, T1 (isointense or hypointense)</p> <p>- Chronic: T1 (hypointense cavity with CSF characteristics).</p>	<ul style="list-style-type: none"> - white matter hyperintensities - Lacunes

Name of Material/ Equipment	Company	Catalog Number	Comments/Description
dcm2niix	N/A	N/A	free download https://github.com/rordenlab/dcm2niix
ITK-SNAP	N/A	N/A	free download www.itksnap.org
MATLAB	MathWorks	N/A	Version 2015a or higher
MRICron	N/A	N/A	free download https://www.nitrc.org/projects/mricron
RegLSM	N/A	N/A	free download www.metavcimap.org/support/software-tools
SPM12b	N/A	N/A	free download https://www.fil.ion.ucl.ac.uk/spm/



1 Alewife Center #200
Cambridge, MA 02140
tel. 617.945.9051
www.jove.com

ARTICLE AND VIDEO LICENSE AGREEMENT

Title of Article:	LESION-SYMBOL MAPPING: A PRACTICAL TUTORIAL FOR BRAIN INFARCT SEGMENTATION AND REGISTRATION ON MRI OR CT
Author(s):	BIESBROEK, KUIJT, WEAVER, ZHIO, DUCKING, BIESSELS

Item 1: The Author elects to have the Materials be made available (as described at <http://www.jove.com/publish>) via:

☒ Standard Access

☐ Open Access

Item 2: Please select one of the following items:

☒ The Author is **NOT** a United States government employee.

☐ The Author is a United States government employee and the Materials were prepared in the course of his or her duties as a United States government employee.

☐ The Author is a United States government employee but the Materials were NOT prepared in the course of his or her duties as a United States government employee.

ARTICLE AND VIDEO LICENSE AGREEMENT

1. **Defined Terms.** As used in this Article and Video License Agreement, the following terms shall have the following meanings: “**Agreement**” means this Article and Video License Agreement; “**Article**” means the article specified on the last page of this Agreement, including any associated materials such as texts, figures, tables, artwork, abstracts, or summaries contained therein; “**Author**” means the author who is a signatory to this Agreement; “**Collective Work**” means a work, such as a periodical issue, anthology or encyclopedia, in which the Materials in their entirety in unmodified form, along with a number of other contributions, constituting separate and independent works in themselves, are assembled into a collective whole; “**CRC License**” means the Creative Commons Attribution-Non Commercial-No Derivs 3.0 Unported Agreement, the terms and conditions of which can be found at: <http://creativecommons.org/licenses/by-nc-nd/3.0/legalcode>; “**Derivative Work**” means a work based upon the Materials or upon the Materials and other pre-existing works, such as a translation, musical arrangement, dramatization, fictionalization, motion picture version, sound recording, art reproduction, abridgment, condensation, or any other form in which the Materials may be recast, transformed, or adapted; “**Institution**” means the institution, listed on the last page of this Agreement, by which the Author was employed at the time of the creation of the Materials; “**JoVE**” means MyJoVE Corporation, a Massachusetts corporation and the publisher of The Journal of Visualized Experiments; “**Materials**” means the Article and / or the Video; “**Parties**” means the Author and JoVE; “**Video**” means any video(s) made by the Author, alone or in conjunction with any other parties, or by JoVE or its affiliates or agents, individually or in collaboration with the Author or any other parties, incorporating all or any portion

of the Article, and in which the Author may or may not appear.

2. **Background.** The Author, who is the author of the Article, in order to ensure the dissemination and protection of the Article, desires to have the JoVE publish the Article and create and transmit videos based on the Article. In furtherance of such goals, the Parties desire to memorialize in this Agreement the respective rights of each Party in and to the Article and the Video.

3. **Grant of Rights in Article.** In consideration of JoVE agreeing to publish the Article, the Author hereby grants to JoVE, subject to **Sections 4 and 7** below, the exclusive, royalty-free, perpetual (for the full term of copyright in the Article, including any extensions thereto) license (a) to publish, reproduce, distribute, display and store the Article in all forms, formats and media whether now known or hereafter developed (including without limitation in print, digital and electronic form) throughout the world, (b) to translate the Article into other languages, create adaptations, summaries or extracts of the Article or other Derivative Works (including, without limitation, the Video) or Collective Works based on all or any portion of the Article and exercise all of the rights set forth in (a) above in such translations, adaptations, summaries, extracts, Derivative Works or Collective Works and (c) to license others to do any or all of the above. The foregoing rights may be exercised in all media and formats, whether now known or hereafter devised, and include the right to make such modifications as are technically necessary to exercise the rights in other media and formats. If the “Open Access” box has been checked in **Item 1** above, JoVE and the Author hereby grant to the public all such rights in the Article as provided in, but subject to all limitations and requirements set forth in, the CRC License.

ARTICLE AND VIDEO LICENSE AGREEMENT

4. **Retention of Rights in Article.** Notwithstanding the exclusive license granted to JoVE in **Section 3** above, the Author shall, with respect to the Article, retain the non-exclusive right to use all or part of the Article for the non-commercial purpose of giving lectures, presentations or teaching classes, and to post a copy of the Article on the Institution's website or the Author's personal website, in each case provided that a link to the Article on the JoVE website is provided and notice of JoVE's copyright in the Article is included. All non-copyright intellectual property rights in and to the Article, such as patent rights, shall remain with the Author.

5. **Grant of Rights in Video – Standard Access.** This **Section 5** applies if the "Standard Access" box has been checked in **Item 1** above or if no box has been checked in **Item 1** above. In consideration of JoVE agreeing to produce, display or otherwise assist with the Video, the Author hereby acknowledges and agrees that, Subject to **Section 7** below, JoVE is and shall be the sole and exclusive owner of all rights of any nature, including, without limitation, all copyrights, in and to the Video. To the extent that, by law, the Author is deemed, now or at any time in the future, to have any rights of any nature in or to the Video, the Author hereby disclaims all such rights and transfers all such rights to JoVE.

6. **Grant of Rights in Video – Open Access.** This **Section 6** applies only if the "Open Access" box has been checked in **Item 1** above. In consideration of JoVE agreeing to produce, display or otherwise assist with the Video, the Author hereby grants to JoVE, subject to **Section 7** below, the exclusive, royalty-free, perpetual (for the full term of copyright in the Article, including any extensions thereto) license (a) to publish, reproduce, distribute, display and store the Video in all forms, formats and media whether now known or hereafter developed (including without limitation in print, digital and electronic form) throughout the world, (b) to translate the Video into other languages, create adaptations, summaries or extracts of the Video or other Derivative Works or Collective Works based on all or any portion of the Video and exercise all of the rights set forth in (a) above in such translations, adaptations, summaries, extracts, Derivative Works or Collective Works and (c) to license others to do any or all of the above. The foregoing rights may be exercised in all media and formats, whether now known or hereafter devised, and include the right to make such modifications as are technically necessary to exercise the rights in other media and formats. For any Video to which this **Section 6** is applicable, JoVE and the Author hereby grant to the public all such rights in the Video as provided in, but subject to all limitations and requirements set forth in, the CRC License.

7. **Government Employees.** If the Author is a United States government employee and the Article was prepared in the course of his or her duties as a United States government employee, as indicated in **Item 2** above, and any of the licenses or grants granted by the Author hereunder exceed the scope of the 17 U.S.C. 403, then the rights granted hereunder shall be limited to the maximum

rights permitted under such statute. In such case, all provisions contained herein that are not in conflict with such statute shall remain in full force and effect, and all provisions contained herein that do so conflict shall be deemed to be amended so as to provide to JoVE the maximum rights permissible within such statute.

8. **Protection of the Work.** The Author(s) authorize JoVE to take steps in the Author(s) name and on their behalf if JoVE believes some third party could be infringing or might infringe the copyright of either the Author's Article and/or Video.

9. **Likeness, Privacy, Personality.** The Author hereby grants JoVE the right to use the Author's name, voice, likeness, picture, photograph, image, biography and performance in any way, commercial or otherwise, in connection with the Materials and the sale, promotion and distribution thereof. The Author hereby waives any and all rights he or she may have, relating to his or her appearance in the Video or otherwise relating to the Materials, under all applicable privacy, likeness, personality or similar laws.

10. **Author Warranties.** The Author represents and warrants that the Article is original, that it has not been published, that the copyright interest is owned by the Author (or, if more than one author is listed at the beginning of this Agreement, by such authors collectively) and has not been assigned, licensed, or otherwise transferred to any other party. The Author represents and warrants that the author(s) listed at the top of this Agreement are the only authors of the Materials. If more than one author is listed at the top of this Agreement and if any such author has not entered into a separate Article and Video License Agreement with JoVE relating to the Materials, the Author represents and warrants that the Author has been authorized by each of the other such authors to execute this Agreement on his or her behalf and to bind him or her with respect to the terms of this Agreement as if each of them had been a party hereto as an Author. The Author warrants that the use, reproduction, distribution, public or private performance or display, and/or modification of all or any portion of the Materials does not and will not violate, infringe and/or misappropriate the patent, trademark, intellectual property or other rights of any third party. The Author represents and warrants that it has and will continue to comply with all government, institutional and other regulations, including, without limitation all institutional, laboratory, hospital, ethical, human and animal treatment, privacy, and all other rules, regulations, laws, procedures or guidelines, applicable to the Materials, and that all research involving human and animal subjects has been approved by the Author's relevant institutional review board.

11. **JoVE Discretion.** If the Author requests the assistance of JoVE in producing the Video in the Author's facility, the Author shall ensure that the presence of JoVE employees, agents or independent contractors is in accordance with the relevant regulations of the Author's institution. If more than one author is listed at the beginning of this Agreement, JoVE may, in its sole

ARTICLE AND VIDEO LICENSE AGREEMENT

discretion, elect not take any action with respect to the Article until such time as it has received complete, executed Article and Video License Agreements from each such author. JoVE reserves the right, in its absolute and sole discretion and without giving any reason therefore, to accept or decline any work submitted to JoVE. JoVE and its employees, agents and independent contractors shall have full, unfettered access to the facilities of the Author or of the Author's institution as necessary to make the Video, whether actually published or not. JoVE has sole discretion as to the method of making and publishing the Materials, including, without limitation, to all decisions regarding editing, lighting, filming, timing of publication, if any, length, quality, content and the like.

12. **Indemnification.** The Author agrees to indemnify JoVE and/or its successors and assigns from and against any and all claims, costs, and expenses, including attorney's fees, arising out of any breach of any warranty or other representations contained herein. The Author further agrees to indemnify and hold harmless JoVE from and against any and all claims, costs, and expenses, including attorney's fees, resulting from the breach by the Author of any representation or warranty contained herein or from allegations or instances of violation of intellectual property rights, damage to the Author's or the Author's institution's facilities, fraud, libel, defamation, research, equipment, experiments, property damage, personal injury, violations of institutional, laboratory, hospital, ethical, human and animal treatment, privacy or other rules, regulations, laws, procedures or guidelines, liabilities and other losses or damages related in any way to the submission of work to JoVE, making of videos by JoVE, or publication in JoVE or elsewhere by JoVE. The Author shall be responsible for, and shall hold JoVE harmless from, damages caused by lack of sterilization, lack of cleanliness or by contamination due to

the making of a video by JoVE its employees, agents or independent contractors. All sterilization, cleanliness or decontamination procedures shall be solely the responsibility of the Author and shall be undertaken at the Author's expense. All indemnifications provided herein shall include JoVE's attorney's fees and costs related to said losses or damages. Such indemnification and holding harmless shall include such losses or damages incurred by, or in connection with, acts or omissions of JoVE, its employees, agents or independent contractors.

13. **Fees.** To cover the cost incurred for publication, JoVE must receive payment before production and publication of the Materials. Payment is due in 21 days of invoice. Should the Materials not be published due to an editorial or production decision, these funds will be returned to the Author. Withdrawal by the Author of any submitted Materials after final peer review approval will result in a US\$1,200 fee to cover pre-production expenses incurred by JoVE. If payment is not received by the completion of filming, production and publication of the Materials will be suspended until payment is received.

14. **Transfer, Governing Law.** This Agreement may be assigned by JoVE and shall inure to the benefits of any of JoVE's successors and assignees. This Agreement shall be governed and construed by the internal laws of the Commonwealth of Massachusetts without giving effect to any conflict of law provision thereunder. This Agreement may be executed in counterparts, each of which shall be deemed an original, but all of which together shall be deemed to be one and the same agreement. A signed copy of this Agreement delivered by facsimile, e-mail or other means of electronic transmission shall be deemed to have the same legal effect as delivery of an original signed copy of this Agreement.

A signed copy of this document must be sent with all new submissions. Only one Agreement is required per submission.

CORRESPONDING AUTHOR

Name:

J.m. BIESBROEK

Department:

NEUROLOGY AND NEUROSURGERY

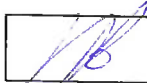
Institution:

UNIVERSITY MEDICAL CENTER UTRECHT

Title:

MD PhD

Signature:



Date:

4 - JAN - 2019

Please submit a **signed** and **dated** copy of this license by one of the following three methods:

1. Upload an electronic version on the JoVE submission site
2. Fax the document to +1.866.381.2236
3. Mail the document to JoVE / Attn: JoVE Editorial / 1 Alewife Center #200 / Cambridge, MA 02140

Response to the editorial comments:

1. The editor has formatted the manuscript to match the journal's style. Please retain the same.

Response: done

2. Please address specific comments marked in the manuscript.

Response: the comments have been addressed. Please see the version of the manuscript with the tracked changes and the original comments of the editor.

3. For the protocol section, please remove the redundancy and make each step crisper. Please use imperative tense throughout the protocol section. Please ensure you answer the how question: how is this step performed.

Response: done

4. Please ensure that the protocol consists of only action steps which direct the reader to do something.

Response: done

5. Once done, please ensure that the protocol is no more than 10 pages and the highlight is no more than 2.75 pages including headings and spacings. This is our hard cut limit. The highlighted steps should form a cohesive narrative with a logical flow from one highlighted step to the next.

Response: done

6. Please explain the representative result in the context of the technique you performed, how did it help you to conclude what you wanted to.

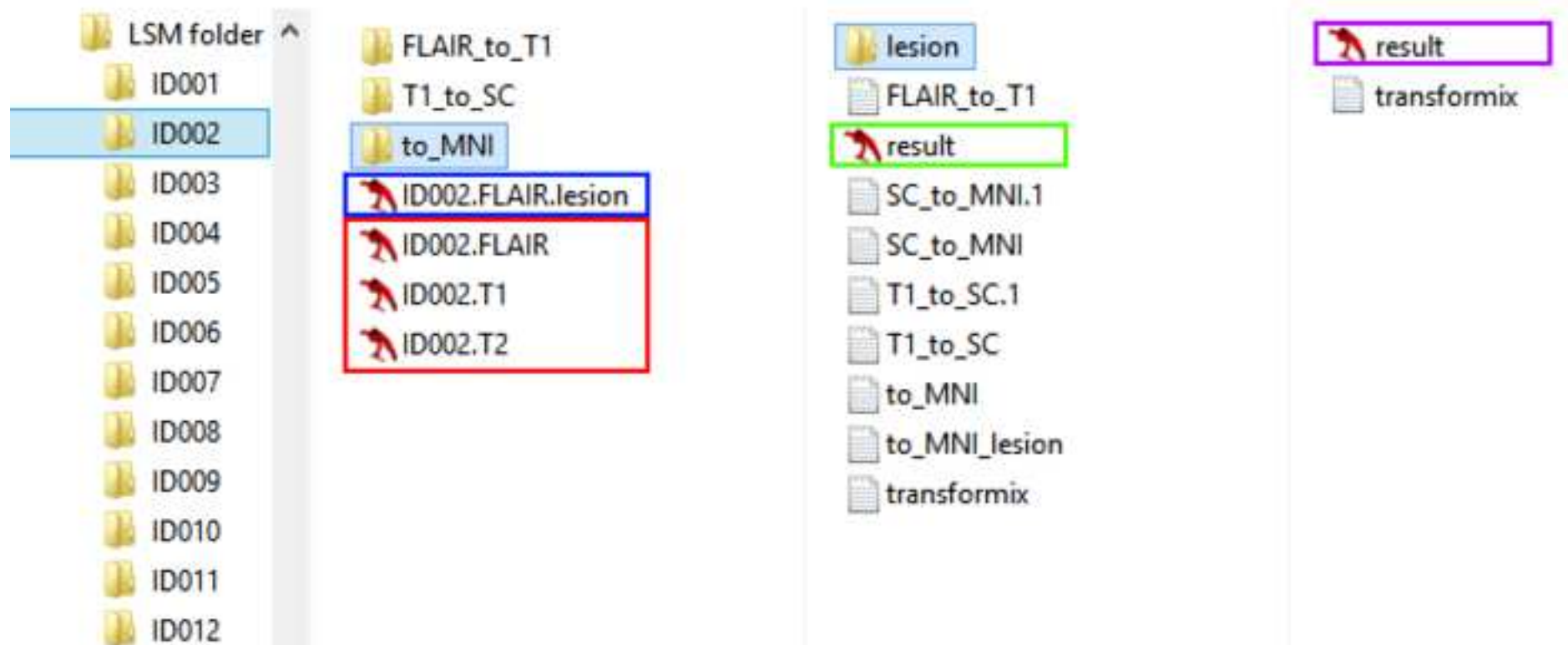
Response: done

7. Figures: Please change "hours" to h. Please leave a single space between numbers and units.

Response: done

8. Once done please proofread the manuscript well for any grammar or spelling errors.

Response: done



Supplementary Figure 1. Typical folder structure during image processing for lesion-symptom mapping. The first subfolder for subject ID002 contains three native scans in nifti format (FLAIR, T1 and T2, in red box) and the segmentation of the FLAIR sequence (in blue box). The three subfolders are created during the registration process by RegLSM. The subfolder to_MNI contains the registered segmented scan (in this case the FLAIR, in green box). The subsequent subfolder contains the registered lesion map in standard space (purple box). Of note, RegLSM will be made BIDS-compatible in the upcoming update.